GPM/DPR Level-2

Algorithm Theoretical Basis Document

Authors: Toshio Iguchi, Shinta Seto, Robert Meneghini,

Naofumi Yoshida, Jun Awaka, Takuji Kubota

December 2010

TABLE OF CONTENTS

1. OBJECTIVES

The objective of the level 2 DPR algorithms is to generate from the level 1 DPR products radar-only derived meteorological quantities on an instantaneous FOV (field of view) basis. A subset of the results will be used by the level 2 combined radar-radiometer algorithm and the level 3 combined and radar-only products.

The general idea behind the algorithms is to determine general characteristics of the precipitation, correct for attenuation and estimate profiles of the precipitation water content, rainfall rate and, when dual-wavelength data are available, information on the particle size distributions in rain and snow. It is particularly important that dual-wavelength data will provide better estimates of rainfall and snowfall rates than the TRMM PR data by using the particle size information and the capability of estimating, even in convective storms, the height at which the precipitation transitions from solid to liquid.

2. BACKGROUND INFORMATION

2.1 HISTORICAL PERSPECTIVE

The Dual-Frequency Precipitation Radar (DPR) on the GPM core satellite will be the second space-borne precipitation radar, following the first such radar, the Precipitation Radar (PR), launched on the TRMM satellite in November, 1997. The TRMM PR has already revolutionized the measurement of precipitation from space by providing high resolution 3-dimentional rain echoes in the tropics and subtropics. The DPR consists of Ku-band (13.6GHz) and Ka-band (35.5GHz) channels. A major source of error in the rainfall estimates from the TRMM/PR comes from the uncertainty in the conversion of radar reflectivity into rainfall rate. This uncertainty originates in the variations of the raindrop size distribution (DSD) that changes by region, season and rain type. One of the reasons for adding the Ka-band frequency channel to the DPR is to provide information on the DSD that can be obtained from non-Rayleigh scattering effects at the higher frequency.

Another reason for the new Ka-band channel is to provide more accurate estimates of the phase-transition height in precipitating systems. This information is very important not only in increasing the accuracy of rain rate estimation by the DPR itself, but in improving rain estimation by passive microwave radiometers.

The third reason for the Ka-band channel arises from the fact that the GPM core satellite will provide coverage up to about 65 degrees latitude; by increasing the sensitivity of this channel, a larger fraction of snow events will be detected.

Since the Ku-band channel of the DPR is very similar to the TRMM PR, the principal challenge in the development of the DPR level 2 algorithms is to combine the new Ka-band data with the Ku-band data to achieve the objectives mentioned above.

2.2 INSTRUMENT CHARACTERISTICS

The DPR consists of the Ku-band precipitation radar and the Ka-band precipitation radar. They are abbreviated as KuPR and KaPR, respectively. These Earth-pointing KuPR and KaPR instruments will provide rain sensing over both land and ocean, both day and night. The KuPR and KaPR design specifications, with all active phased array elements functioning, are shown in Table 2.2-1. The spacecraft orbital information is shown in Table 2.2-2.

Table 2.2-1 DPR Design Specification

Item	**KuPR**	**KaPR**
Swath Width	245 kilometers (km)	120 kilometers (km)
Range Resolution	250 meters (m)	250/500 meters (m)
Spatial Resolution	5.2 km (Nadir at the height of 407 km)	5.2 km (Nadir at the height of 407 km)
Beam Width	0.71 degrees (Center Beam)	0.71 degrees (Center Beam)
Transmitter	128 Solid State Amplifiers	128 Solid State Amplifiers
Peak Transmit Power[3]	1012.0 Watts (W)	146.5 Watts (W)
Pulse Repetition Freq.[1]	4000 to 4500 Hertz (Hz)	4000 to 4500 Hertz (Hz)
Pulse Width	two 1.6 microseconds (μs) pulses	two 1.6 microseconds (μs) pulses in matched beams two 3.2 microseconds (μs) pulses in interlaced scans
Beam Number	49	49 (25 in matched beams and 24 in interlaced scans)
Minimum measurable rain rate	0.5 mm/h	0.2 mm/h
Beam matching error	Under 1000 m	
Observable range	19km to Surface (to -5 km near nadir)	19km to Surface (to -5 km near nadir)
Dynamic range	From -5dB below the system noise level to +5dB above the nominal maximum surface echo level	From -5dB below the system noise level to +5dB above the nominal maximum surface echo level
Receiver power accuracy	+/- 1dB	+/- 1dB
Scan Angle (in Observation Mode)	±17° Cross Track	±8.5° Cross Track
Frequencies	13.597 and 13.603 GHz	35.547 and 35.553 GHz

Bandwidth	14 MHz	14 MHz
Max. Mass	472 kilograms (kg)	336 kilograms (kg)
Power (max)	446 W (orbit average)	344 W (orbit average)
Science Data Rate (max)	109 kilobits per second (kbps) (The Total of KuPR and KaPR is 190 kbps)	81 kilobits per second (kbps) (The Total of KuPR and KaPR is 190 kbps)
Housekeeping Data Rate (nominal)[2]	1 kilobits per second (kbps)	1 kilobits per second (kbps)

1. In nominal operation mode.

2. 1 kbps may increase up to 2 kbps during SCDP switch-overs.

3. This parameter is for informational purposes in the ICD.

Table 3.1-2 Spacecraft Orbital Information

Inclination	65°
Mean semi-major axis	6776.14 km
S/C Altitude Control Box	± 1 km
Orbit Eccentricity	0.00010 (0-0.0005 tolerance)
Geodetic Altitude Variation Range	397 km to 419 km

Figure 3.1-1 shows the DPR scan pattern. KuPR's scan pattern is similar to that of the TRMM PR. It has 49 footprints in a scan and the footprint size is about 5 km in diameter. The scan swath is 245 km. The KaPR also has 49 footprints, but these are divided into two types of scan. In the first type of scan (Ka_MA), the beams are matched to the central 25 beams of KuPR, providing a swath of 120 km. In the second type of scan (Ka_HS), the KaPR is operated in the high-sensitivity mode to detect light rain and snow; in this case, its beams are interlaced within the scan pattern of the matched beams as shown in Fig. 3.1-1. The KuPR and KaPR for the Ka_MA scan have the same range resolution (250 m), while the range resolution of data in Ka_HS is 500m. In both cases, radar echoes are over-sampled at twice the rate of the corresponding resolution: 125 m for the matched beams and 250 m for the Ka_HS.

Figure 3.1-2 shows the observation range. The DPR's echo sampling is designed to cover a range that, at minimum, extends from the surface to 19 km above the sea level (or from the Ellipsoid). The pulse repetition interval is adjusted according to the satellite altitude and the angle of observation. As a result, the number of independent samples changes slightly as a function of the scan angle.

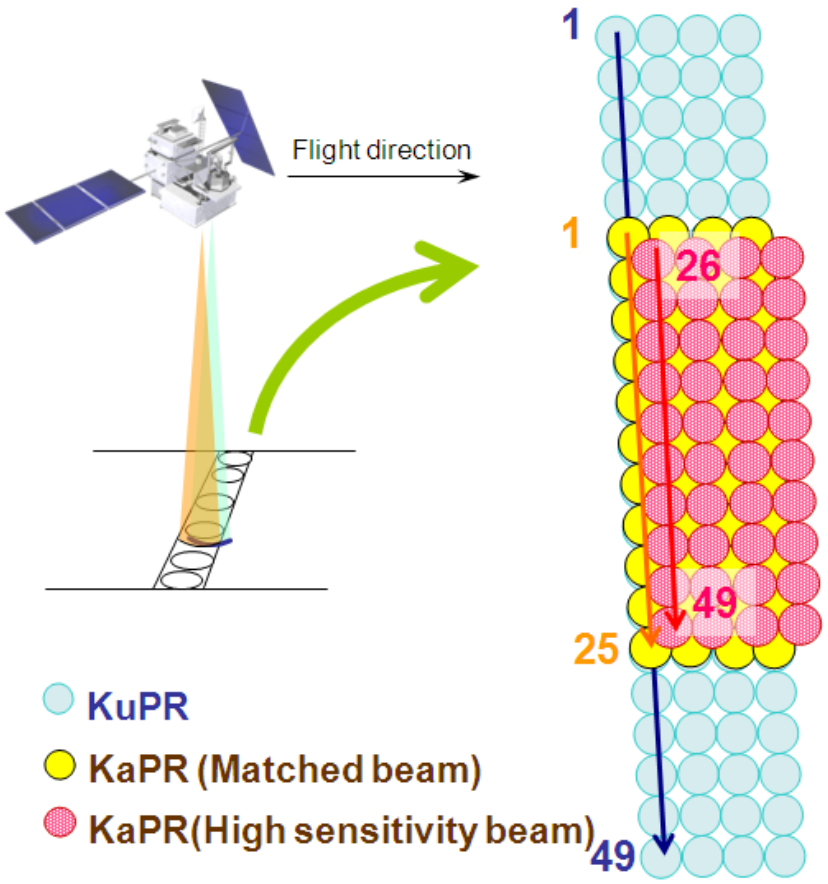

Figure 3.1-1. DPR scan pattern.

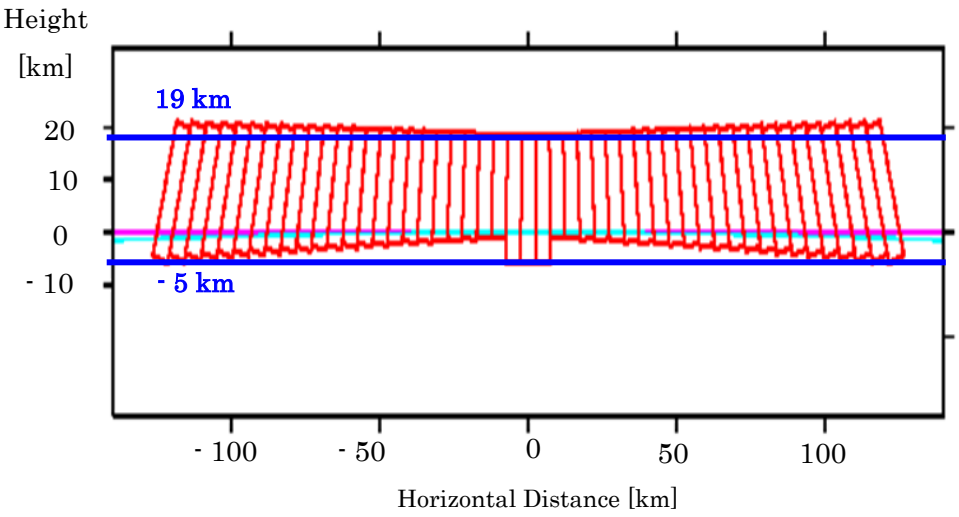

Figure 3.1-2 DPR's data sampling range

3. ALGORITHM DESCRIPTION

3.1. Theoretical Description

3.1.1. Physical Basis of the Algorithm

The radar transmits a pulse of radio waves and receives an echo from an object. The object in the case of precipitation radar is a distribution of rain drops in the volume defined by the antenna directivity, the pulse width and the time between the transmission and the reception of the pulse. The received power P_r from rain at range r is proportional to the apparent radar reflectivity factor $Z_{m0}(r)$.

$$P_r(r) = \frac{C\,|K|^2}{r^2} Z_{m0}(r), \tag{3-1}$$

where C is the radar constant, and K is a constant defined as a function of refractive index m of scattering particles by the following equation.

$$K = \frac{m^2 - 1}{m^2 + 2}. \tag{3-2}$$

When the radar electric specifications and range r are given, Z_{m0} can be calculated. Therefore, we can assume that $Z_{m0}(r)$ can be derived from a measurement of the echo power. Z_{m0} is related to the effective radar reflectivity factor Z_e by

$$Z_{m0}(r) = A(r) Z_e(r) \tag{3-3}$$

where A is the attenuation factor. The effective radar reflectivity factor Z_e can be expressed in terms of the backscattering cross section $\sigma_b(D)$ of a precipitation particle of diameter D and the particle size distribution $N(D)$:

$$Z_e = \frac{\lambda^4}{\pi^5\,|K|^2} \int \sigma_b(D) N(D) dD \tag{3-4}$$

Here λ is the wavelength of the electromagnetic waves, and

Rainfall rate R can also be expressed in terms of $N(D)$,

$$R = \int V(D) v(D) N(D) dD, \tag{3-5}$$

where $V(D)$ is the volume of the precipitation particle of diameter D, $v(D)$ is its falling velocity.

If $N(D)$ could be characterized by a single parameter, for example D^*, then Z_e and D^* would be in one-to-one correspondence. Since R and D^* is in a one-to-one correspondence as well, once Z_e is obtained, then $N(D)$ could be specified by D^* corresponding to this Z_e, and R could be calculated. In this case, therefore, the attenuation correction used to obtain Z_e from Z_{m0} is the primary problem to be solved. This is the principle of rain estimation for a single frequency radar such as the TRMM PR.

In fact, however, variations of $N(D)$ in nature cannot be characterized sufficiently by a single parameter in many cases. As a result, rain estimates from a single frequency radar often involve errors and biases.

In contrast, variations in $N(D)$ can be well represented by two parameters as far as the conversion from Z_e

to R is concerned. If rain is measured by the radar at two wavelengths and if one of the wavelengths divided by 2π is smaller than or comparable to the average raindrop size, then the corresponding backscattering cross section will deviate from that of Rayleigh scattering, and Z_e at this wavelength differs from Z_e at the longer wavelength where Rayleigh scattering generally applies. This situation enables us to estimate two parameters of the model function of $N(D)$ and results in a better estimate of rainfall rate. This is the idea of rainfall estimation with a dual-wavelength radar. In other words, if $N(D)$ is characterized by two parameters N^* and D^*, Z_e at two wavelengths Z_{e1} and Z_{e2} become functions of N^* and D^*,

$$Z_{e1}(N^*, D^*) = \frac{\lambda_1^4}{\pi^5 |K|^2} \int \sigma_{b1}(D) N(D; N^*, D^*)\, dD \tag{3-6}$$

$$Z_{e2}(N^*, D^*) = \frac{\lambda_1^4}{\pi^5 |K|^2} \int \sigma_{b2}(D) N(D; N^*, D^*)\, dD \tag{3-7}$$

Once Z_{e1} and Z_{e2} are given, we can solve (3-6) and (3-7) for N^* and D^*, and R can be calculated from $N(D;N^*,D^*)$.

As in the single-wavelength case, the attenuation corrections to obtain Z_{e1} and Z_{e2} at two frequencies from measured or apparent radar reflectivities Z_{m1} and Z_{m2} are crucial. Since the major attenuation comes from precipitation itself, and the DSD parameters can be estimated from Z_{e1} and Z_{e2}, we look for a profile of pairs of DSD parameters (one pair per range gate) that gives the attenuation corrected profiles of Z_{e1} and Z_{e2} that are consistent with the attenuations caused by the precipitation particles whose size distributions are characterized by these DSD parameters. This part of the algorithm is the heart of the rainfall retrieval with dual-frequency radar data. Details of the algorithm are described below.

Attenuation caused by non-precipitation particles and atmospheric gases must be compensated for beforehand. Specifically, we need to take into account the attenuation caused by cloud water, water vapor and oxygen molecules. Meteorological data and storm models are planned to be used to estimate their profiles for this purpose.

(1) Effective radar reflectivity factor Z_e, specific attenuation k and measured radar reflectivity factor

The effective radar reflectivity factor Z_e is given by (3-4). Similarly, the specific attenuation k is given in terms of the drop size distribution $N(D)$ and the total extinction cross section $\sigma_e(D)$ by

$$k = c_k \int \sigma_e(D) N(D) dD\,, \tag{3-8}$$

where $c_k = \dfrac{0.01}{(\ln 10)}$ if k is expressed in [dB (km^{-1})], $\sigma_e(D)$ in [mm^2], and $N(D)$ in [mm^{-1} m^{-3}].

Let r [km] denote the distance from the radar along the range. The measured radar reflectivity factor $Z_{m0}(r)$ [mm^6 m^{-3}] involves the attenuation by precipitation particles $A_P(r)$ and by non-precipitation particles $A_{NP}(r)$ as is expressed in the following equation.

$$Z_{m0}(r) = Z_e(r)A_{NP}(r)A_P(r) = Z_e(r)A_{NP}(r)\exp\left[-0.2(\ln 10)\int_0^r k(s)ds\right], \quad (3\text{-}9)$$

where s is a dummy variable. Equation (3-9) can be rewritten in decibels as shown below.

$$10\log_{10} Z_{m0}(r) = 10\log_{10} Z_e(r) + 10\log_{10} A_{NP}(r) - 2\int_0^r k(s)ds\,. \quad (3\text{-}10)$$

After attenuation correction for non-precipitation particles, $Z_{m0}(r)$ becomes $Z_m(r)$, where $Z_m(r)$ is given by.

$$Z_m(r) = Z_{m0}(r)A_{NP}(r)^{-1} = Z_e(r)A_P(r)\,. \quad (3\text{-}11)$$

By substituting Eq. (3-11) into Eq. (3-9), the following equation is obtained.

$$10\log_{10} Z_m(r) = 10\log_{10} Z_e(r) - 2\int_0^r k(s)ds\,. \quad (3\text{-}12)$$

(3) HB method

Let us assume a power-law relation between k and Z_e as shown below.

$$k(r) = \alpha(r)Z_e(r)^{\beta}, \quad (3\text{-}13)$$

where α and β are coefficients, α can be range dependent, but β should be constant along the range.

With the help of Eq. (3-13), Eq. (3-12) can be solved for Z_e and written in the form of (3-14),

$$Z_e(r) = \frac{Z_m(r)}{\left[1 - 0.2(\ln 10)\beta\int_0^r \alpha(s)Z_m(s)^{\beta}ds\right]^{1/\beta}}, \quad (3\text{-}14)$$

Alternatively, the equation can be solved for the attenuation factor, A_p, giving,

$$A_P(r) = \left[1 - 0.2(\ln 10)\beta\int_0^r \alpha(s)Z_m(s)^{\beta}ds\right]^{1/\beta}. \quad (3\text{-}15)$$

(4) Path integrated attenuation (PIA)

Here, Path Integrated Attenuation (PIA) is defined as integrated attenuation caused by precipitation particles from the radar to the surface. If $r=r_s$ at the surface, PIA is given as shown below.

$$\mathrm{PIA} = -10\log_{10} A_P(r_s) = 2\int_0^{r_s} k(s)ds\,. \quad (3\text{-}16)$$

Eq. (3-12) can be rewritten as a function of the PIA.

$$10\log_{10} Z_m(r) = 10\log_{10} Z_e(r) - \mathrm{PIA} + 2\int_r^{r_s} k(s)ds\,. \quad (3\text{-}17)$$

By substituting Eq. (3-15) at $r=r_s$ into Eq. (3-16), the following equation is obtained.

$$\mathrm{PIA} = -\frac{10}{\beta}\log_{10}\left[1 - 0.2(\ln 10)\beta\int_0^{r_s} \alpha(s)Z_m(s)^{\beta}ds\right]. \quad (3\text{-}18)$$

The PIA can be estimated by taking the difference between the surface backscattering cross

sections with and without precipitation (surface reference technique).

(5) Parameterization of drop size distribution function

From a mathematical point of view, $N(D)$ should be parameterized with at most two unknown parameters in order to characterize $N(D)$ deterministically from dual-frequency measurements. To keep the discussion fairly general, $N(D)$ is parameterized in the following way.

$$N(D) = N^* n(D; D^*), \tag{3-19}$$

where N^* and D^* are unknown parameters and n is a function of D. By substituting Eq. (3-19) into Eq. (3-4) and (3-8), Z_e and k are given as below.

$$Z_e = N^* I_b(D^*), \quad I_b(D^*) = \frac{\lambda^4}{\pi^5 |K|^2} \int \sigma_b(D) n(D; D^*) dD \tag{3-20}$$

$$k = N^* I_e(D^*), \quad I_e(D^*) = \frac{0.01}{(\ln 10)} \int \sigma_e(D) n(D; D^*) dD \tag{3-21}$$

which shows that Z_e and k can be decomposed into N^* and a function of D^* ($I_b(D^*)$ and $I_e(D^*)$).

(6) Retrieval

(6-1) Dual-frequency retrieval

If Z_m is available at two frequencies,

$$10\log_{10} Z_{m1}(r) = 10\log_{10} N^*(r) + 10\log_{10} I_{b1}(D^*(r)) - 2\int_0^r k_1(N^*(s), D^*(s))\, ds \tag{3-22}$$

$$10\log_{10} Z_{m2}(r) = 10\log_{10} N^*(r) + 10\log_{10} I_{b2}(D^*(r)) - 2\int_0^r k_2(N^*(s), D^*(s))\, ds \tag{3-23}$$

The third term of the right hand side of Eq. (3-22) or (3-23) is equal to the 2-way attenuation from the storm top to range r, which implies that the retrieval should be performed sequentially from the top range bin to the gate of interest. This attenuation can be treated as a known quantity if the attenuation is expressed as a function of the DSD parameters derived at each gate. Since the solution progresses from the storm top downwards, the method is called the forward retrieval method.

If an independent estimate of the PIA is available, in addition to Z_m,

$$10\log_{10} Z_{m1}(r) = 10\log_{10} N^* + 10\log_{10} I_{b1}(D^*) - PIA + 2\int_r^{r_s} k_1(s) ds \tag{3-24}$$

$$10\log_{10} Z_{m2}(r) = 10\log_{10} N^* + 10\log_{10} I_{b2}(D^*) - PIA + 2\int_r^{r_s} k_2(s) ds \tag{3-25}$$

Eqs. (3-24) and (3-25) instead of Eq. (3-22) and (3-23) can be used. In this case, the fourth term of the right hand side of Eq. (3-24) or (3-25) is equal to the 2-way attenuation from the gate of interest (at range r) to the surface, implying that the retrieval should be done sequentially from the

bottom range bin to gate of interest. As in the forward method, if the attenuation is related to the DSD parameters at each range gate, the third term can be treated as known. This method is called backward retrieval method. In reality, because of ground clutter, the third term cannot be calculated without the some assumption regarding the profile of the precipitation in the clutter region. Also, because PIA estimates by the SRT have some error, then Eq. (32) differs from Eq. (31), and the backward retrieval method yields different solutions from the forward retrieval method. However, the backward retrieval method is preferable, as it gives numerically stable and unique solutions, while the forward retrieval method usually has two solutions at each range bin.

In the backward retrieval method, we define $10\log_{10}Z_{b1}$ and $10\log_{10}Z_{b2}$ by moving the third and fourth term of the right hand side to the left hand side in Eqs. (3-24) and (3-25).

$$10\log_{10} Z_{b1} \equiv 10\log_{10} Z_{m1} + \mathrm{PIA}_1 - 2\times\int_r^{r_s} k_1(s)ds = 10\log_{10} N^* + 10\log_{10} I_b(D^*) \tag{3-26}$$

$$10\log_{10} Z_{b2} \equiv 10\log_{10} Z_{m2} + \mathrm{PIA}_2 - 2\times\int_r^{r_s} k_2(s)ds = 10\log_{10} N^* + 10\log_{10} I_b(D^*)\,. \tag{3-27}$$

By taking the difference between Eqs. (3-26) and (3-27), we obtain:

$$10\log_{10} Z_{b1} - 10\log_{10} Z_{b2} = 10\log_{10} I_{b1}(D^*) - 10\log_{10} I_{b2}(D^*)\,, \tag{3-28}$$

As the left hand side of Eq. (3-28) is known, D^* can be derived. For liquid precipitation, the right-hand side of (3-28) has a maximum, and Eq. (3-28) has generally two solutions.

(7-2) Single-frequency retrieval

If Z_m is available only at a single frequency, we need to characterize $N(D)$ with a single parameter. This means that we assume a relationship between N^* and D^*. Once such a relation is assumed, we can translate the N^*-D^* relation to the k-Z_e relation, and the attenuation correction can be carried out by Eq. (3-14). If a PIA estimate by SRT ($\mathrm{PIA_{SRT}}$) is substituted into PIA in Eq. (3-18), the equality is generally not satisfied. This inequality is caused either by an error in the SRT or by an error in the k-Z_e relation. If the SRT is correct, the k-Z_e relation can be modified to $k=\varepsilon\alpha Z_e^{\beta}$ where ε satisfies Eq. (3-29). This is called the ε-adjustment method.

$$\mathrm{PIA_{SRT}} = -\frac{10}{\beta}\log_{10}\left[1 - 0.2(\ln 10)\beta\varepsilon\int_0^{r_s}\alpha(s)Z_m(s)^{\beta}\,ds\right] \tag{3-29}$$

Once the ε parameter is found from (3-29), the Hitschfeld-Bordan solution with the modified k-Z_e relation provides the attenuation-corrected radar reflectivities.

From the above attenuation correction process, k and Z_e are obtained. Then, by taking the ratio of Eq. (3-20) to Eq. (3-21), D^* can be retrieved.

$$\frac{k}{Z_e} = \frac{I_e(D^*)}{I_b(D^*)} \tag{3-30}$$

Generally, the right hand side of Eq. (3-30) is a monotonic function of D^* so that Eq. (3-30) has a unique solution. Since $N(D)$ is characterized by a single parameter, there is one-to-one correspondence between Z_e and D^* or k and D^*, and we can directly calculate D^* as well.

3.1.2. Overall structure of the algorithm

(1) Algorithms

There are three kinds of Level 2 algorithms for the DPR: DPR algorithm, Ku-only (KuPR) algorithm, and Ka-only (KaPR) algorithm. The latter two are signle-frequency (SF) algorithms. The DPR algorithm is a dual-frequency (DF) algorithm.

The DF algorithm employs both KuPR and KaPR L1B standard products as inputs. The DF algorithm cannot be executed unless both L1B products are available. Pixels observed by DPR can be categorized into three types: pixels in the inner swath of normal scans (observed both by KuPR and KaPR), pixels in the outer swath of normal scans (observed only by KuPR), and pixels in the interleaved scans (observed only by KaPR in the high-sensitivity mode). The KuPR algorithm is executed for pixels in both inner and outer swaths of normal scans. The KaPR algorithm is executed for pixels in the inner swath of normal scans and in the interleaved scans. The DF algorithm is executed for pixels of all the three kinds.

In the DF algorithm, pixels in the inner swath of normal scans are categorized into the dual-beam (DB) pixels. The other pixels in the DF algorithm and all the pixels in the SF algorithms are categorized into the single-beam (SB) pixels. For a SB pixel, the DF algorithm can use data in dual-frequency observations at neighboring pixels, while the SF algorithms can use data only in the corresponding single-frequency observations. For example, by using the characteristics of the drop size distribution estimated by dual-frequency measurements at DB pixels in the inner swath, the DF algorithm can give better estimates at SB pixels in outer swath than the KuPR algorithm.

Each algorithm executes data for one orbit at a time. For an orbit, only after the two SF algorithms are properly executed, the DF algorithm will be executed. The order of execution between the KuPR algorithm and the KaPR algorithm is not fixed. The algorithms are designed in such a way that the order of execution for different orbits has no restrictions within the same calendar month, but one month of data should be executed as a unit to produce proper databases.

(2) Input/Output Files

The input and output files of the KuPR, KaPR and DF algorithms are as follows.

<u>KuPR algorithm</u>

(Input) KuPR L1B standard product, Weather data file, Database file

(Output) KuPR L2 standard product, KuPR L2 temporary file, KuPR L2 environment data

<u>KaPR algorithm</u>

(Input) KaPR L1B standard product, Weather data file, Database file

(Output) KaPR L2 standard product, KaPR L2 temporary file, KaPR L2 environment data

<u>Dual-frequency algorithm</u>

(Input) KuPR L2 standard product, KaPR L2 standard product, KuPR L2 temporally file, KaPR

L2 temporary file, Database file, KuPR L2 environment data, KaPR L2 environment data
(Output) DPR L2 standard product, DPR L2 environment data, DPR L2 temporary file

The temporary files include some results of the SF algorithms, which are not written in the standard products. The temporary products can be treated as research products, once the DPR L2 standard product and other outputs are properly produced by the DF algorithm.

The environmental data include the profiles of atmospheric parameters assumed in the L2 algorithm. Because of its large volume, the ancillary environmental data are output into a separate file from the standard product.

The weather data file is prepared by converting the resolution and/or variables of weather analysis/reanalysis/forecast dataset in advance to L2 algorithm.

Database files and database update files are explained later.

An asterisk (*) indicates that the files may not be necessary as input of the DF algorithm, because information in these files are copied to KuPR/KaPR L2 temporary files/standard products.

(3) Modules

The framework of the L2 algorithm is shown in the figure. This framework is common to the KuPR, KaPR, and DF algorithms. The main module manages the overall procedure, and it employs seven sub-modules.

The main module will open and close files, call sub-modules, and read/write all the input and output files and variables. It will also terminate the algorithm.

Sub-modules can read/write files and variables as long as they are permitted. As a basic rule, they should process for all the pixels in the orbit, and the order of pixels processed is not fixed (can be determined by each module). Sub-modules cannot call other sub-modules. When a sub module is terminated, the processing is returned to the main module.

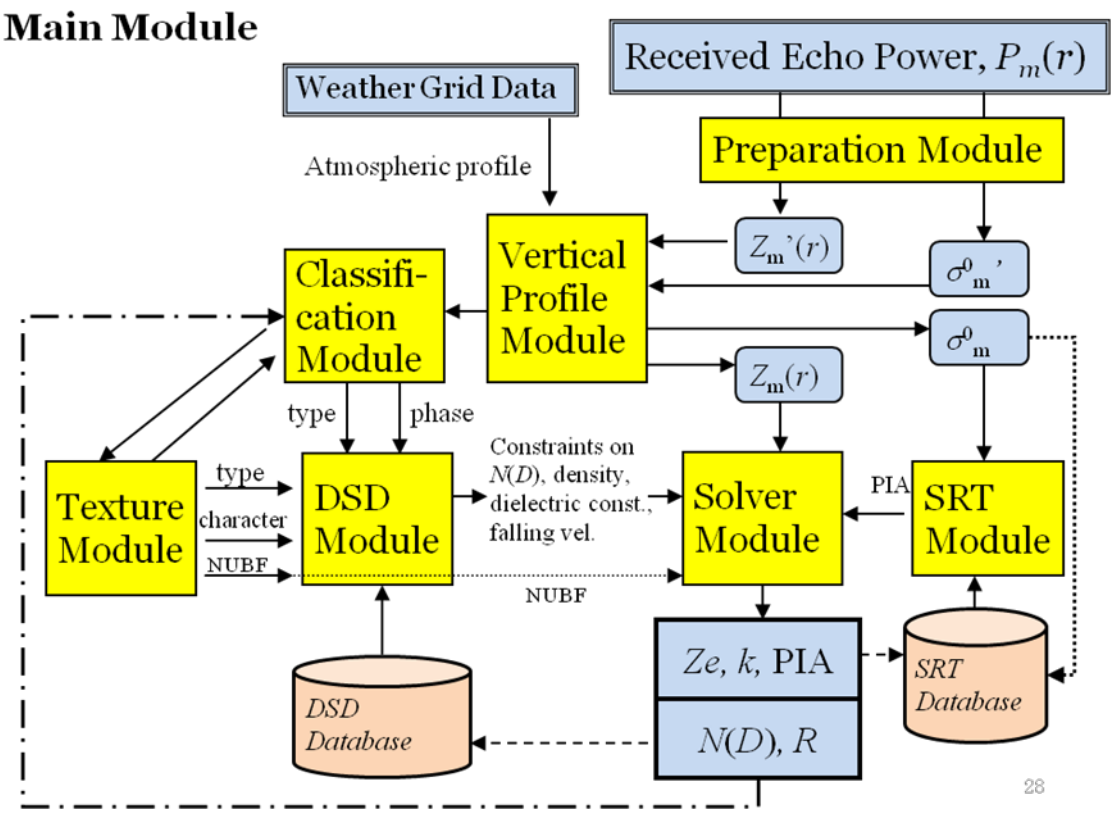

(4) Basic roles of the modules

The L2 algorithm is to numerically solve Eq. (3-22) or (3-23) for DB pixels and Eq. (3-30) for SB pixels to obtain N^* and D^*. The retrieval process is carried out in the Solver module, but the preparation of equations is shared by the other six modules. The PIA in Eqs. (3-29), (3-24) and (3-25) can be estimated in the SRT module. The DSD module is responsible for quantifying the terms in the equations such as α, β, $n(D, D^*)$, $I_b(D^*)$, and $I_e(D^*)$ based on the physical characteristics of precipitation (precipitation types and bright band information) determined by the Classification module. Z_m is converted from Z_{m0} through attenuation correction for non-precipitation particles in the Vertical Profile module and Z_{m0} is converted from received echo power in the Preparation module.

(5) Variables

A tentative table of variables is attached to this document. The table is used for all the three algorithms in the L2 algorithms. There are two types of variables: L1B variables and L2 variables. L1B variables are just copied from the L1B standard products. L2 variables are somehow processed in the L2 algorithms. Not all but some selected variables are written in L2 standard, temporary, or environment products.

A variable with scan dependence, angle bin dependence, range bin dependence, and

frequency dependence is expressed as an array in the source code. Some variables may have other dimensions than scan, angle bin, range bin, and frequency. Type (bytes) of a variable can be changed when it is written into the product to save the file size.

Some variables can take different values in the SF algorithms and DF algorithm. Those variables are product dependent. Product dependence and frequency dependence are explained by examples below.

- "Location of observation" is without product dependence and without frequency dependence.
- "Measured radar reflectivity factor Z_{m0}" is without product dependence and with frequency dependence.
- "Equivalent radar reflectivity factor Z_e" is with product dependence and with frequency dependence.

In the DF algorithm, variables with product dependence should be reprocessed, but variables without product dependence can be copied from SF products. Variables without product dependence and without frequency dependence should take the same value in KuPR product and KaPR product, but there is some possibility of disagreement as the KuPR algorithm and KaPR algorithm are processed independently. In the case of disagreement, a rule (e.g. KuPR algorithm is more reliable) should be prepared to determine the value in the DF algorithm.

(6) Databases

A database is to include useful information for the algorithm, and exists as separate files from the main body of the algorithm (source code). For example, the SRT database is used in the SRT module to increase the accuracy of the PIA estimates. The L2 algorithm can refer to and update databases. The actual updating process is done not by directly modifying the database file, but by creating an intermediate file. The intermediate files are summarized and the database file is modified off line.

(7) Look-up tables

A look-up table has a similar role with a database, but the difference is that a look-up table will basically not be updated. Therefore, we can treat the look up tables as part of the main body of the algorithm, and do not list the look-up tables as input and output files. The L2 algorithm employs a DSD look-up table and a RTM look-up table in the DSD module and the Solver module, respectively.

3.2 Modules

3.2.0 Main module

The basic procedure of the main module is described in (1) below. At first, it is necessary to run the algorithm in the basic procedure, but in near future, advanced procedures described in (2) and (3) should be tested.

(1) The basic procedure

In the basic procedure, sub-modules are executed in the following order, and each module is called only once.

Firstly, the Preparation module is executed. This module judges the existence of precipitation, and identifies the precipitation pixels.

Secondly, the Vertical profile module is executed. The ancillary atmospheric profile data are used to correct for the attenuation caused by non-precipitation particles to obtain the surface backscattering cross sections both at precipitation and no-precipitation pixels.

Thirdly, the Classification module classifies each precipitation pixel into an appropriate storm type. At no-precipitation pixels, almost no processes are taken.

Fourthly, the SRT module is executed. At no-precipitation pixels, SRT database is updated based on the measurement of surface backscattering cross sections. Note that the SRT module can be executed anytime after the Vertical profile module and before the Solver module.

Finally, the Solver module is executed. At no-precipitation pixels, almost no processes are taken.

(2) Advanced procedure

By executing some of the modules multiple times, improvement of results is expected. Two kinds of examples are given below.

(2-1) Recursive procedure

Once the basic procedure is done, the same procedure is repeated again with the parameters estimated in the first cycle. In the second cycle, for example, we can estimate the attenuation due to cloud liquid water by referring the precipitation rate estimated in the first cycle.

(2-2) Parallel procedure

In the basic procedure, the sub-modules are required to determine the values of variables in charge, but sometimes they do not have enough information to estimate the values in a deterministic way. A parallel procedure allows a sub-module to give multiple estimates and to let the following sub-modules execute with multiple estimates. For example, if the precipitation type is not determined with confidence in Classification module, then the following (DSD and Solver) modules are executed with multiple assumptions of precipitation types, and the main module checks which

assumption gives the vertical profiles of Z_e and the corresponding precipitation rate R in accordance with the assumed precipitation type. Thus, the precipitation type can be determined afterwards.

(3) Additional processes

Some important processes may be missing in the basic procedure, for example, non-uniform beam filling (NUBF) correction. They should be involved in the final version of the algorithm, but currently, it has not been determined which modules are in charge of additional processes; NUBF correction can be done inside the Solver module, or should be shared with the DSD module and/or the SRT module, or a new module (Texture module) should be introduced.

3.2.1 Preparation module

1. Objectives and functions of the Preparation Module (PREP)

The primary purposes of the preparation module are (1) to classify the pixels into either rain or no-rain pixels, (2) to convert the received power P_r into measured reflectivity factor Z_m' without any attenuation corrections at each range bin, and (3) to calculate apparent normalized surface cross section $\sigma^0{}_m'$ without any attenuation correction at each pixel.

2. Algorithm descriptions of the PREP

In this section, the preparation module of Ku-band level-2 algorithm will be described in detail. As to the preparation module of Ka-band level-2 algorithm, it is almost the same with that for the Ku-band. The DPR level-2 algorithm can use level-2 products and level-2 supplementary products of both Ku-only and Ka-only algorithms. As a result, it can provide necessary information to other modules of the DPR level-2 algorithm without re-calculations.

Reading of input data

The module reads data from a Ku-band level-1B product that includes not only the radar echoes but also other variables related to the measurements such as scan time (ScanTime), footprint position (Latitude, Longitude), local zenith angle (scLocalZenith), operational mode (operationalMode, acsMode), elevation (DEMHmean), data quality flag (dataQuality). In the case of the DPR level-2 algorithm, the module reads level-2 products and level-2 supplementary products of both Ku-band and Ka-band algorithms.

Status confirmation

The module refers to dataQuality of level-1B product scan by scan. If dataQuality is bad (not 0), level-2 values of the corresponding scan are overwritten by missing values.

Calculation of range distance (rangeDist)

The range distance (rangeDist) is defined by the distance from the satellite to each range bin along the radar beam. Each rangeDist is calculated from the range distance from the satellite to the highest range bin (startBinRange), the number of range bins with normal sampling (echoLowResBinNumber), the number of range bins with over-sampling (echoHighResBinNumber) and the range bin size (rangeBinSize). Specifically, the range distance (rangeDist) for normal sampling ranges are calculated by using the following equation.

$$rangeDist = R_0 + (n-1)\times \Delta R \qquad (n = 1, 2, 3, \cdots, N)$$

The rangeDist for over sampling ranges are

$$rangeDist = R_0 + \{N + (m-1)\}\times \Delta R \qquad (m = 1, 2, 3, \cdots, M)$$

where R_0 = startBinRange in L1B product

N = echoLowResBinNumber in L1B product

M = echoHighResBinNumber in L1B product

ΔR = rangeBinSize in L1B product

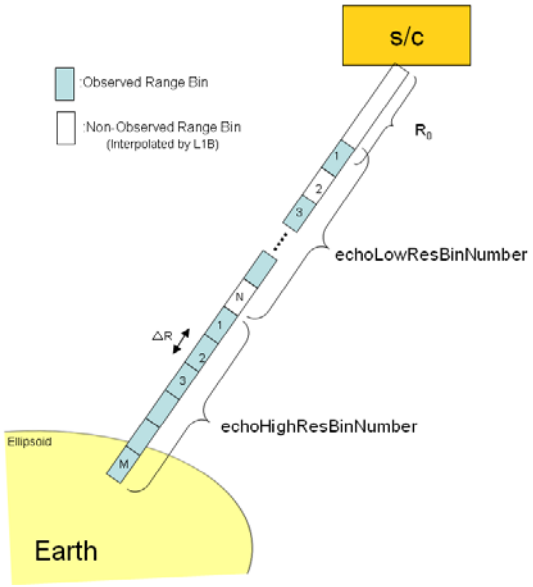

Figure 3.2.1-1 Definition of rangeDist

Calculation of height (Height)

The height is defined by the vertical distance from the footprint of radar beam on the Ellipsoid to the range bin in question. In order to calculate Height, we define ellipsodiBinOffset as follows.

ellipsoidBinOffset = scRangeEllipsoid - { R_0 + (binEllipsoid-1) x rangeBinSize }

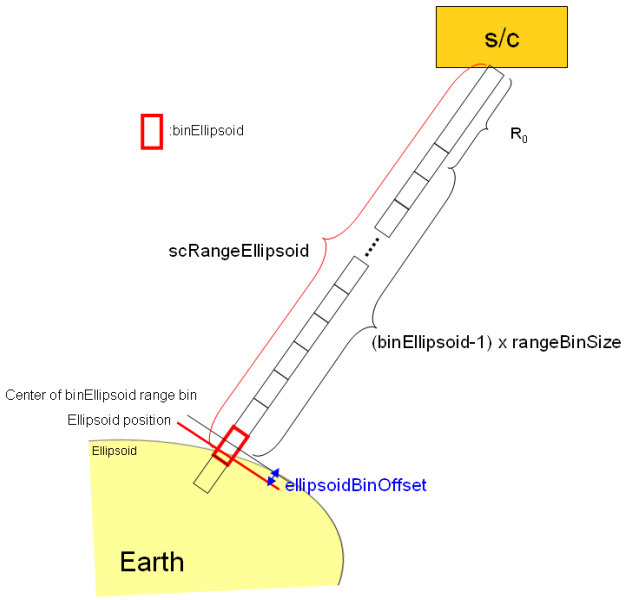

Figure 3.2.1-2 Definition of ellipsodiBinOffset

Then, Height of a binRangeNo (as shown "p" in figure 3.2.1-3) is calculated by the following equation.

Height[binRangeNo]

= {(binRangeNo - binEllipsoid_2A25) x rangeBinSize + ellipsoidBinOffset }

x cos(localZenithAngle)

where binEllipsoid_2A25 is the Ellipsoid range bin number in level2.

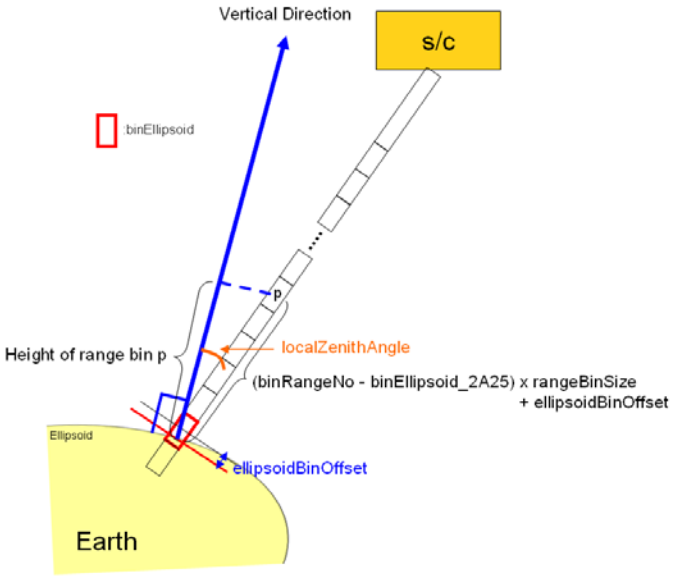

Figure 3.2.1-3 Definition of Height

Extraction of level-1B range data

echoPower and echoFlag of level-1B product are given at each range bin. The array size of data with range-bin dependence in Ku level-1B is 260. The array sizes of data with range-bin dependence in Ka_MA and Ka_HS level-1B are 260 and 130, respectively. On the other hand, the array size of data with range-bin dependence in Ku level-2 is 200 in the algorithm calculation. As to the array sizes for range bins of Ka_MA and KA_HS level-2 are 200 and 100, respectively. The preparation module renumbers the range bins relative to the Ellipsoid position in level-2 so that the range bin number at the Ellipsoid becomes 176 (88) in the Ku and Ka_MA level-2 (of Ka_HS) products. The top and bottom range bins of level-2 are defined as follows.

rangeBottom = binEllipsoid@L1B + 24 for Ku, Ka_MA

(rangeBottom = binEllipsoid@L1B + 12 for Ka_HS)

rangeTop = binEllipsoid@L1B - (200-1) + 24 for Ku, Ka_MA

(rangeTop = binEllipsoid@L1B - (100-1) + 12 for Ka_HS)

Thus, at the nadir angle bin, data from -3 km to +22 km altitude relative to the Ellipsoid are extracted.

Land surface type (landSurfaceType)

The land-and-ocean flag (landOceanFlag) of level1B product gives land, ocean, inland water, and coast classification for each footprint. The preparation module adds surface type information for land and coast area, using footprint position (Latitude and Longitude) and an external data base. The surface type information is stored in landSurfaceType.

Surface detection (binRangeRealSurface)

The preparation module determines the surface range bin using the received power (echoPower), and DEM related data, such as binDEM, scRangeDEM, DEMHmean, binDEMHtop, binDEMHbottom of level-1B product. The estimated surface position is stored in binRangeRealSurface.

Estimation of Clutter-free bottom (rangeClutterFreeBottom)

The range bin number of the clutter-free bottom is estimated using echoPower profiles. binRangeRealSurface may be used as a reference of the search window. The clutter-free bottom range bin number is stored in rangeClutterFreeBottom.

Calculation of Signal power (echoSignalPower)

Calculations of signal power are applied to all range bin data except missing data which are flagged by dataQuality in L1B product.

Pecho = pow(10.0,(double) echoPower /10)

Pnoise = pow(10.0,(double) noisePower /10)

Psignal = Pecho - P noise

echoSignalPower = $10*\log_{10}$(Psignal)

where echoPower and noisePower are stored in dB unit in L1B product.

If Psignal values are negative, missing value is stored in echoSignalPower.

Rain/NoRain classification (flagEcho, flagPrecip, binStormTop, heightStormTop)

Rain/NoRain classification is carried out in two steps. At first, it is done for all range bins above the rangeClutterFreeBottom except missing data which are labeled by dataQuality in L1B product. If echoSignalPower exceeds a certain threshold, it means that rain is detected for the range bin. The results of Rain/NoRain classification for range bins are stored in flagEcho. The sidelobe clutter range bins shall be detected and overwrite flagEcho with a clutter value in this function.

Then, using the surrounding flagEcho results, the Rain/NoRain classification for angle bin is carried out for all angle bins except missing data. The results of Rain/NoRain classification for each angle bin are stored in flagPrecip. The modules in the downstream in the flow chart may use the flagPrecip to

determine the target pixels for processing.

The function also detects a highest rain position in each angle bin and provides binStormTop and heightStormTop.

Calculation of Z_m' factor (zFactorMeasured)

Z_m' is defined as the measured reflectivity factor without any attenuation corrections. Z_m' is calculated using a radar equation at all range bins above the rangeClutterFreeBottom except missing data which are labeled by dataQuality in L1B product. The result of Z_m' is stored in zFactorMeasured. The radar equation is as follows.

$$P_r = C \cdot P \cdot L_r \cdot E$$

$$= [Pt \cdot Gat \cdot Gar] \cdot \left[\left(\frac{\lambda}{4\pi r} \right)^4 \cdot \frac{4\pi}{\lambda^2} \right] \cdot L_r \cdot \left[\frac{\pi^5}{\lambda^4} \cdot |K|^2 \cdot Ze \cdot 10^{-18} \cdot c\tau \cdot \frac{\pi r^2 \theta_{0a} \theta_{0c}}{2^4 (\ln 2)} \right]$$

$$= \frac{\pi^3 \cdot c}{2^{10} \cdot 10^{18} \cdot (\ln 2)} \cdot \frac{Pt \cdot Gat \cdot Gar \cdot \theta_{0a} \theta_{0c} \cdot \tau \cdot |K|^2}{\lambda^2 r^2} \cdot L_r \cdot Ze$$

In the preparation module, Z_m' (=Lr・Ze) is calculated by using the following equation.

$$P_r = \frac{\pi^3 \cdot c}{2^{10} \cdot 10^{18} \cdot (\ln 2)} \cdot \frac{Pt \cdot Gat \cdot Gar \cdot \theta_{0a} \theta_{0c} \cdot \tau \cdot |K|^2}{\lambda^2 r^2} \cdot Zm'$$

$$Zm' = \frac{2^{10} \cdot 10^{18} \cdot (\ln 2)}{\pi^3 \cdot c} \cdot \frac{\lambda^2 \cdot r^2 \cdot P_r}{Gat \cdot Gar \cdot \theta_{0a} \theta_{0c} \cdot \tau \cdot |K|^2 \cdot Pt}$$

where

r	range distance *(rangeDist)*
λ	wave length *(eqvWavelength of L1B)*
|K|	function of dielectric constant
Gt	transmitter antenna gain *(txAntGain of L1B)*
Gr	receiver antenna gain *(rxAntGain of L1B)*
θc	Cross-track beam width *(crossTrackBeamWidth of L1B)*
θa	Along-track beam width *(alongTrackBeamWidth of L1B)*
c	light speed
τ	transmitter pulse width *(transPulseWidth of L1B)*
Pt	transmitted power *(radarTransPower of L1B)*
Pr	received signal power *(echoSignalPower)*

It should be noted that |K| is a constant in the preparation module. Any adjustment of |K| by temperature is controlled in the solver module if necessary.

Calculation of σ^0_m' (sigmaZeroMeasured)

σ^0_m' is defined as the measured normalized surface cross section without any attenuation corrections. Calculation of σ^0_m' is done for all footprints except missing data which are labeled by dataQuality in L1B product. The value of σ^0_m' is stored in sigmaZeroMeasured.

$$\sigma^0{}_m'(\theta_z) = P_{rs}(r_0) \cdot \frac{512\pi^2 \ln 2}{P_t \lambda^2 \cdot Gt \cdot Gr} \cdot \frac{losses}{1} \cdot \frac{\cos(\theta_z) \cdot r_0^{\,2}}{\theta a \cdot thbp}$$

where

$$thbp^{-1} = \sqrt{\theta_c^{-2} + thp^{-2}}, \qquad thp^{-1} = \frac{2}{c\tau} \cdot r_0 \cdot \tan(\theta_z)$$

r_0	range distance from the satellite to the geographic surface
θc	Cross-track beam width *(CrossTrackBeamWidth of L1B)*
θa	Along-track beam width *(AlongTrackBeamWidth of L1B)*
Pt	transmitted power *(radarTransPower of L1B)*
Prs	received signal power (*echoSignalPower*)
r_0	range distance from the satellite to the geographic surface *(ref. binRangeRealSurface)*
θz	zenith angle *(localZenithAngle)*
loss	band path filter loss
λ	wave length *(eqvWavelength of L1B)*
Gt	transmitter antenna gain *(txAntGain of L1B)*
Gr	receiver antenna gain *(rxAntGain of L1B)*
c	light speed
τ	transmitter pulse width *(transPulseWidth of L1B)*

3. Interfaces to other algorithms

As to the Ku-band and Ka-band level-2 algorithms, input data for this module is Ku-band and Ka-band level1B product, respectively. For the DPR level-2 algorithm, input data for this module are level-2 products and level-2 supplementary products of both Ku-band and Ka-band. The outputs will be used by the Solver module and other modules in the DPR algorithm.

3.2.2 Vertical Profile Module

Objectives and functions of the Vertical Profile Module (VER)

The primary purposes of the VER are to read ancillary environmental data, to provide vertical profiles of the environmental parameters, to compute the path-integrated attenuation (PIA) due to non-precipitation (NP) particles, and to give radar reflectivity factors corrected for attenuation by the non-precipitation particles. The VER provides environmental information such as pressure, temperature, water vapor, and cloud liquid water at each range bin. The VER calculates the attenuation due to water vapor, molecular oxygen, and cloud liquid water.

For Ku, Ka, Ka_HS, the VER is executed using the information of the pixel lat/lon and the range bin width. For the DPR, results of the Ku, Ka, Ka_HS are introduced.

Algorithm descriptions of the VER

Utilization of ancillary environmental data

The VER inputs ancillary environmental data, objective analysis data by Japan Meteorological Agency (JMA) named as JMA Global Analysis (GANAL) product or reanalysis data by JMA named as Japanese 25-year ReAnalysis (JRA-25) and JMA Climate Data Assimilation System (JCDAS) product (Onogi et al. 2007). By reading the ancillary environmental product, the VER provides pressure, temperature, water vapor, and cloud liquid water for each range bin. In addition, the VER computes a level of 0 degree centigrade and finds out the range bin corresponding to the level of 0 degree centigrade.

The horizontal resolutions of the GANAL JRA-25 and JCDAS are 0.5 and 1.25 degree latitude/longitude, respectively. The pressure levels such as 1000, 925, 850, 700, 600, 500, 400, 300, 250, 200, 150, 100 hPa, and so on are converted to the height levels before the input of the algorithm. The temporal resolution is 6 hourly as 00, 06, 12, and 18Z. The VER inputs two 6-hourly files and compute using linear temporal interpolation. We also use a linear horizontal and vertical interpolation according to pixel lat/lon information and range bin height. Antenna beam directions are ignored and we assume only nadir direction. The VER provides pressure, temperature, water vapor, and cloud liquid water at each range bin.

Calculation of attenuation by water vapor

At a frequency less than 100GHz, the attenuation coefficient due to water vapor, $\kappa_{H2O}(f)$(dB/km) is expressed as follows (Waters 1976, Ulaby et al. 1981, Meneghini and Kozu 1990),

$$\kappa_{H2O}(f) = 2f^2\rho_v\left(\frac{300}{T}\right)^{3/2}\gamma_l\left[\left(\frac{300}{T}\right)e^{-644/T}\frac{1}{\left(494.4-f^2\right)^2+4f^2{\gamma_l}^2}+1.2\times10^{-6}\right],$$

where

f : frequency (GHz)

ρ_v : water vapor content (g/m^3)

γ_l : parameter of line width (GHz)

T : temperature (K)

The line width parameter γ_l is given as

$$\gamma_l = 2.85\left(\frac{P}{1013}\right)\left(\frac{300}{T}\right)^{0.626}\left(1+0.018\frac{\rho_v T}{P}\right),$$

where P : pressure (hPa)

Calculation of attenuation by molecular oxygen

For attenuation by molecular oxygen, the following expression is valid for frequencies less than 45 GHz (Rosenkranz 1975, Ulaby et al. 1981, Meneghini and Kozu 1990).

$$\kappa_{O2}(f) = 1.1\times10^{-2} f^2\left(\frac{P}{1013}\right)\left(\frac{300}{T}\right)^2 \gamma\left[\frac{1}{(f-f_0)^2+\gamma^2}+\frac{1}{f^2+\gamma^2}\right],$$

where

f : frequency (GHz)

$f_0 = 60\ GHz$

γ : parameter of line width (GHz)

T : temperature (K)

Line width parameter γ is given by

$$\gamma = \gamma_0\left(\frac{P}{1013}\right)\left(\frac{300}{T}\right)^{0.85},$$

where

$$\gamma_0 = \begin{cases} 0.59 & 333 \le P\,(hPa) \\ 0.59\left[1+3.1\times10^{-3}(333-P)\right] & 25 \le P < 333\,(hPa) \\ 1.18 & P < 25\,(hPa) \end{cases}$$

Calculation of attenuation by cloud liquid water

For attenuation by cloud liquid water κ_{CLV} over non-precipitation pixels, the cloud water content of the ancillary environmental data product is utilized. In the cloud scheme of the JCDAS, an effective radius of cloud liquid droplets is fixed at 15 microns. In this calculation, we assume cloud particle distribution $n_c(D)$ as mono-disperse, that is,

$$n_c(D) = N_c\delta(D-2r_e)$$

where

D : Diameter

r_e =15 microns

N_c : Number concentration of cloud liquid particles

For cloud liquid water content Q (kg/m^3), N_c is expressed as follows,

$$N_c = \frac{3Q}{4\pi r_e^3 \rho_w}$$

κ_{CLV} is computed due to the Rayleigh scattering using $n_c(D)$.

The mono-disperse assumption implies the homogeneity of the cloud distribution, although clouds generally distribute with high inhomogeneity within the grid-size of the reanalysis such as 1.25-degree latitude/longitude. Therefore, the previous formula will underestimate κ_{CLV} over precipitation pixels. To avoid such an error we will adopt an empirical formula such as in Iguchi et al. (2009) over the precipitation pixels.

Input Variables

Input: from MOSS or PPS

Ancillary environmental data Two 6-hourly files

Surface: Surface pressure, Mean sea level pressure

Pressure levels: Geopotential height, temperature, water vapor, and cloud liquid water

Input: from Preparation Module

Geolocation
scanTime
Elevation
landSurfaceType
localZenithAngle
flagPrecip
rangeRealSurface
rangeStormTop
heightStormTop

rangeClutterFreeBottom

sigmaZeroMeasured

zFactorMeasured

rangeBottom

rangeTop

Height

4. Definitions of Output Variables

airTemperature[80][49] Temperature

rangeZeroDeg[49] Range bin number corresponding to the level of 0 degree centigrade.

heightZeroDeg[49] Height of the level of 0 degree centigrade.

airPressure[80][49] Pressure (hPa)

waterVapor[80][49] Water vapor (kg/m^3)

attenuationNPwv[80][49] Attenuation by water vapor (dB/km)

attenuationNPoxygen[80][49] Attenuation by molecular oxygen (dB/km)

cloudLiquidWater[80][49] Cloud Liquid water content (kg/m^3)

attenuationNPclw[80][49] Attenuation by cloud Liquid water (dB/km)

attenuationNP[80][49] Sum of Attenuations by water vapor, molecular oxygen, and cloud liquid water

$$Atten_{NP}(r) = \kappa_{WV}(r) + \kappa_{O2}(r) + \kappa_{CLW}(r)$$

piaNP[80][49] PIA by the non-precipitation particles.

$$PIA_{NP}(r) = 2\int_0^r Atten_{NP}(s)ds = 2\int_0^r \kappa_{WV}(s) + \kappa_{O2}(s) + \kappa_{CLW}(s)ds$$

zFactoNPCorrected[80][49] Radar reflectivity corrected for attenuation by the non-precipitation particles

$$Z_m(r) = Z_m^{'}(r)/A_{NP}(r)$$
$$A_{NP}(r) = \exp(-qPIA_{NP}(r)) \qquad \text{where} \qquad q = 0.1\ln(10)$$

sigmaZeroNPCorrected[49] σ^0 corrected for attenuation by the non-precipitation particles

$$\sigma^0 = \sigma^{0'}/A_{NP}(r)$$
$$A_{NP}(r = sfc) = \exp(-qPIA_{NP}(r = sfc))$$

5. Intermediate Files

Before the input of the algorithm, the pressure levels of the ancillary environmental data are converted to the height levels. In addition, the attenuations and PIA estimates by water vapor,

molecular oxygen, and cloud liquid water are computed in advance.

6. Description of the Processing Procedure

Before the input of the algorithm, the pressure levels of the ancillary environmental data will be converted to the height levels. In addition, the attenuations and PIA estimates by water vapor, molecular oxygen, and cloud liquid water will be computed in advance.

For Ku, Ka, Ka_HS, the VER is executed using the information of the pixel lat/lon and the range bin width. For the DPR, calculated results of the Ku, Ka, Ka_HS are used.

7. Interfaces to other algorithms:

Input data for this algorithm is from the Preparation Module and Ancillary environmental data; the outputs will be used by the Classification module, DSD module, Solver Module and others.

3.2.3 Classification Module

Introduction

In reliable rain rate retrieval using space-borne radars, information about the drop size distribution (DSD) is necessary. DSD varies depending on the rain type. Therefore, rain type classification plays an important role in the GPM DPR algorithm.

There exist two distinctive rain types, one is stratiform and the other is convective. Stratiform rain is characterized by its weakness in intensity, wide extension in area, and in many cases accompanying a bright band (BB) in radar echo. Because of the last characteristic, detection of a BB can be used for determining stratiform rain.

The rain type classification is made on pixel basis. Hence, the rain type is the same along a radar beam. Then there arises the following ambiguous situation. Suppose that, when the radar reflectivity being examined along a given radar beam, the precipitation echo happens to exist only at altitude higher than 0C height. What is the rain type for this case? Is it stratiform or convective? This is a difficult question to answer. To handle such an ambiguous case, the third category of "other" type will be introduced in a similar manner to the case of the TRMM PR algorithm 2A23. The third category "other" means that there exists only cloud or possibly noise when the radar echo is examined along the radar beam.

A surprise in the early TRMM PR observation was a ubiquitous shallow isolated rain system, which may be warm rain but it still remains a puzzle what it actually is. TRMM PR observation shows that shallow isolated rain is weak, which does not agree with the concept of warm rain which is thought to be very strong. There also exists shallow non-isolated rain, whose statistical properties seem to be very similar to those of shallow isolated rain. Shallow rain (both shallow isolated and shallow non-isolated rain) will be marked by a shallow rain flag, flagShallowRain, which is independent of the rain type flag, typePrecip.

Objectives

The classification (CSF) module detects bright band (BB) and classifies rain into three major categories, which are stratiform, convective, and other.

Algorithm Principles

Rain type classification will be made by a V-method (Vertical profiling method) and by an H-method (Horizontal pattern method) [1][2]. The rain types by the V-method and H-method are unified, and the Classification (CSF) module outputs the unified rain type, which consists of three major categories, stratiform, convective, and other.

In the V-method, detection of BB is made first. Detection of BB will be made by examining the

vertical profile of the radar reflectivity factor (Z) and see if the vertical profile of Z satisfies certain conditions which are typical to the profile of Z when BB exists. When BB is detected, rain type is stratiform if the reflectivity factor in the rain region does not exceed a special convective threshold. When BB is not detected, and the reflectivity factor exceeds a conventional convective threshold, rain type is convective. When rain type is neither stratiform nor convective, the rain type is "other" in the V-method.

In the H-method, a horizontal pattern of a representative radar reflectivity factor is examined. Here the representative reflectivity factor means the maximum value of reflectivity factor in the rain region along the considering radar beam. Rain type is classified using a modified University-of-Washington convective/stratiform separation method [3]. In the H-method, rain type is again classified into three categories: stratiform, convective and other. In the H-method, detection of convective rain is made first. If the rain type is not convective, the rain type is stratiform unless the reflectivity factor is very small, being almost identical to noise. If rain type is neither convective nor stratiform, the rain type is other.

Assumptions

This document describes the dual frequency algorithm only. Single frequency algorithms for the CSF module, that are Ku-band only CSF algorithm and Ka-band only CSF algorithm would easily be obtained by omitting some parts of the dual frequency CSF algorithm.

It is assumed that all the input data to the CSF module are expanded in the CPU memory, hence a direct memory access to all the data is available. In such a memory luxurious case, the CSF module can examine the horizontal extent of relevant quantities, such as radar reflectivity factor, very easily.

Actual Algorithm (Data Processing)

The BB detection is based on a search of typical BB peak in the case of Ku-band by examining the range profile of radar reflectivity along a given antenna beam. In the case of Ka-band, however, since a clear BB peak is not expected, a typical Ka-band BB range profile is detected, for example, by using a template method.

(1) Selection of pixels to be processed:

- Skip the process for the pixel if no precipitation echo exists in Ku-band and Ka-band data. This judgment can be made by examining a flag from the PRE module, flagPrecip.
- Skip the process for the pixel if the quality flag of Ka-band and/or that of Ku-band shows that the pixel is a bad pixel or that the data is missing. This judgment can be made by examining a flag from the PRE module, qualityData.

(It is assumed here that the information about missing data is also available from the qualityData flag.)

(2) Determination of range where precipitation echoes exist:

- Determination of the echo top and the echo bottom, where the echo top is given by rangeStormTop from the PRE module and the echo bottom is given by rangeClutterFreeBottom from the PRE module.

(3) Detection of bright band (BB):

- Set the BB search window using rangeZeroDeg from the VER module. The BB search window ranges from rangeZeroDeg – 4 to rangeZeroDeg + 8 with a 250m interval (TBD), where the center of the BB window is rangeZeroDeg + 2 which is about 0.5 km below the 0 degree height. This window range is reasonable from TRMM PR experience and many other radar observations (unfortunately, Ka-band radar data may not exhibit a clear BB peak, but the BB search window can be the same for the Ku-band and Ka-band). Experience shows that BB peak appears about 0.5 km below the 0 degree height.

Detection of BB will be made using the NP-attenuation corrected radar reflectivity factors, zFactorNPCorrected, from the VER module, where NP-attenuation means attenuation due to non-precipitation particles.

Detection of BB will be made by two methods: one is a vertical method and the other is a (horizontal) texture method. The vertical method examines the profile of radar reflectivity factor. If the profile of the radar reflectivity satisfies certain conditions which characterize BB, it is determined that there exists BB. The above characteristic conditions are different between Ku-band and Ka-band. In the Ku-band, a sharp BB peak should be observed in the profile of radar reflectivity. In the Ka-band, however, a clear BB peak may not be observed, but there must be a detectable characteristic change in the slope in the radar reflectivity profile near the BB.

The (horizontal) texture method detects BB by examining nearby pixels. The (horizontal) texture method is effective for detecting a BB smeared by slanted beam observation.

In the dual frequency algorithm, there is a possibility that BB is detected in Ku-band alone or in Ka-band alone. Even when a BB is detected at both frequencies, there is a possibility that the height of BB disagrees between Ku-band and Ka-band. In such a case, the result of Ku-band should be given a higher priority. Details are TBD.

When BB is detected, the following quantities are computed or given and written to the output of the CSF module.

- flagBB

This flag indicates that BB is detected.

- rangeBBPeak

Range bin of BB peak. In the case of Ku-band, it is simple and straight forward. In the case of Ka-band, BB peak may not be clear, hence further study is required. Details are TBD.

- rangeBBTop

Range bin of BB top, which can easily be obtained in the nadir beam provided that the BB

peak is clear. The definition of rangeBBtop for a smeared BB needs further study. Details are TBD.

- rangeBBbottom

Range bin of BB bottom, which can easily be obtained in the nadir beam provided that the BB peak is clear. The definition of rangeBBbottom for a smeared BB needs further study. Details are TBD.

- heightBB

Height of BB which corresponds to rangeBBPeak. The heighBB can be obtained using Height from the PRE module.

- widthBB[39]

Width of BB. At the nadir direction, widthBB can be computed simply by

(rangeBBBottom - rangeBBTop)* (range bin interval)

At off-nadir directions, empirical correction will be made so that the width of BB is consistent with that at the nadir direction. Details are TBD.

- qualityBB

Quality flag of BB detection. Details are TBD.

(4) Rain type classification

Rain type classification will be made by two method: one is V-method and the other is H-method. Both methods classify rain into three categories; stratiform, convective and other. The rain types by the two methods are unified, and the CSF module will output the unified rain type, which also consists of three major categories; stratiform, convective and other.

An internal flag, qualityTypePrecip, will be prepared for the purpose of recording the quality of rain type classification.

(4-1) V-method

In the V-method, stratiform rain is detected first.

- When BB is detected, the rain type is stratiform.
- When BB is not detected, the rain type is convective if one of the following (tentative) conditions is satisfied. Otherwise, the rain type is other.

(a) The radar reflectivity factor, zFactorNPCorrected, in the valid range between rangeStormTop and rangeClutterFreeBottom exceeds a threshold, which is 40 dBZ in Ku-band and 40 dBZ (TBD value) in Ka-band.

(b) Storm top in Ka- or Ku-band is very high (> 15 km (TBD)).

In the V-method, detection of shallow rain is also made independently of the above mentioned rain type classification. When the following condition is satisfied in both Ka- and Ku-bands, it is judged as

shallow rain, which will be marked by an internal flag:

heightStormTop < heightZeroDeg – matrgin (TBD)

(4-2) H-method

In the H-method, horizontal texture of the maximum value of zFactorNPCorrected in the rain region along each radar beam, Zmax, is examined. A modified University of Washington convective/stratiform separation method is applied to the horizontal extent of Zmax. When one of the following conditions is satisfied, the considering pixel is a convective center:

(a) Zmax in the pixel exceeds a convective threshold, or

(b) Zmax in the pixel stands out against that in the surrounding area.

Rain type of the convective center is convective, and the rain type of pixels adjacent to the convective center is convective.

If the rain type is not convective, and if Zmax is not small enough to be considered as noise, the rain type is stratiform. If Zmax is very small, being almost identical to noise, the rain type is other.

In the H-method, a rain having small cell size is also detected. The rain having small cell size will be classified as convective.

In the H-method, shallow rain is separated out into shallow isolated and shallow non-isolated by examining the horizontal extent of shallow rain.

(4-3) Unification of rain type

Rain types by the V-method and by the H-method are unified, and the CSF module will output the unified rain type, which consists of three major categories of stratiform, convective and other. The unified rain type will be written to the flag typePrecip.

There will be many rain type sub-categories depending on the combination of V- and H-mehod results. The numbering system of typePrecip is TDB. However, the numbering of typePrecip will be made in such a way that by a simple rule the major rain types can be extracted.

(4-4) Detection of orographic rain (optional)

In the CSF module, detection of orographic rain will be tried. Unfortunately, however, detection of orographic rain would require research works. Until coming up with a workable algorithm for detecting orographic rain, an internal flag is prepared but the content of the flag is set to the default value of ‘orographic rain not detected’.

When orographic rain is detected, the result will be reflected in the unified rain type flag typePrecip.

Use of attenuation corrected Z from SLV

The use of attenuation corrected radar reflectivity factor Z, zfactorCorrected, from the SLV module would

be preferable for the detection of convective rain. The most simple approach would be to re-evaluate the rain types by running a simplified CSF module after all the output of SLV is available, which implies a sequential data processing. If such a sequential processing is allowed, re-evaluation of rain types can be implemented easily. If the sequential processing is not allowed, however, a sophisticated use of memory access to the data would be necessary.

For re-evaluating the rain types, a simplified CSF module would be adequate because detection of BB would not strongly be affected by the use of zfactorCorrected since detection of BB examines the shape Z profile but not the value of Z itself. The use of zfactorCorrected would affect the detection of convective rain, because the strength of Z is used for the detection of convective rain. Hence, for re-evaluating rain types using
zfactorCorrected, BB detection can be skipped. Shallow rain detection can also be skipped. There would be other parts which can be skipped.

The simplified CSF module would use the following data:

zfactorCorrected（from SLV）
rangeStormTop（from PRE）
rangeClutterFreeBottom（from PRE）
rangeZeroDeg（from VER）
flagBB（from CSF）
rangeBBBottom（from CSF）
typePrecip (from CSF)

Among these, the last typePrecip would be overwritten by the simplified CSF module, which would be prepared separately from the fully-equipped CSF module.

It would be preferable to store typePrecip from the fully-equipped CSF module using a different name such typePrecip_0.

Input and Output Variables

Input Variables

From Preparation (PRE) module:

lat
lon
ScanTime information (Year, Month, DayOfMonth, Hour, Minute, Second,
Millisecond, DayOfYear, SecondOfDay)
elevation
landSurfaceType
localZenithAngle
flagPrecip

binRealSurface
binStormTop
heightStormTop
binClutterFreeBottom
sigmaZeroMeasured
rangeBottom
rangeTop
Height
echoSignalPower

From Vertical (VER) module:
airTemperature
binZeroDeg
zFactorNPCorrected
heightZeroDeg
flagEcho (R/W) (This flag marks possible sidelobe clutter positions.)
qualityData (R/W)

Output Variables

flagBB [4 byte integer (can be 2byte integer)]
binBBPeak [4 byte integer]
binBBTop [4 byte integer]
binBBBottom [4 byte integer]
heightBB [4 byte real (or integer)]
widthBB [4 byte real (or integer)]
qualityBB [4 byte integer (can be 2 byte integer)]
typePrecip [4 byte integer]
qualityTypePrecip [4 byte integer (can be 2 byte integer)]
flagShallowRain [4 byte integer (can be 2 byte integer)]

Relation to other modules

The Classification (CSF) module uses data from the Preparation (PRE) module and the vertical (VER) module. The output data from the CSF module will be used by the Solver (SLV) module.

For re-evaluating the rain types, a simplified CSF module would be used.

3.2.4 DSD module

(1) Objective

The primary objective of DSD module is to set the physical variables of precipitation particles (especially, density, dielectric constants, and falling velocity), to parameterize $N(D)$ (in other words, to set $n(D; D^*)$), and to set k-Z_e relation (its parameters α and β).

(2) Processes

The following processes are almost common to SB pixel and DB pixel.

(2-1) Target pixels and range bins

Pixels with precipitation and without any errors are processed. Range bins from the storm top range bin to the land surface range bin (including those without precipitation and those with ground clutter) are processed. In case of DB pixel, range bins from higher storm top range bin between the two frequencies to lower land surface range bin between the two frequencies are processed below.

(2-2) Nodes and the physical temperature and phase of the particles

Five range bins are selected and assigned to node-A to node-E as below. Simultaneously, the physical temperature of particles (particle temperature) and the phase of particles are set. Particle temperature will be used to calculate the dielectric constants and it is not necessary the same with air temperature. The procedure of setting is dependent on the precipitation types and the detection of bright band.

(2-2-1) Stratiform precipitation with bright band

A range bin at the upper edge of bright band is assigned to node-B, a range bin at the peak of bright band is node-C, and a range bin at the lower edge of bright band is node-D. Between node-B and node-D, particle temperature is set to be 0^oC. Above node-B, particle temperature is set so that the difference between particle temperature and air temperature is the same with that at node-B. Below node-D, particle temperature is set so that the difference between particle temperature and air temperature is the same with that at node-D. A range bin with particle temperature is closest to -15^oC is assigned to node-A, and a range bin with particle temperature is closest to 20^oC is node-E.

At and above node-A, the phase of precipitation is *Solid*. At and below node-D, the phase of precipitation is *Liquid*. At other range bins, below node-A and above node-D, the phase of precipitation is *Mixed* (Solid and Liquid).

(2-2-2) Stratiform precipitation without bright band

The process is the same as (2-2-1), but the nodes-B, C, D are set as follows.

A range bin corresponding to 0 degree C height is assigned to node-C. A range bin which is higher than node-C by 750m is node-D and a range bin which is lower than node-C by 750m is node-D.

(2-2-3) Convective precipitation or other-type precipitation

The process is the same as (2-2-2), but the phase is set as below.

At and above node-A, the phase of precipitation is *Solid*. At and below node-C, the phase of precipitation is *Liquid*. At other range bins, below node-A and above node-D, the phase of precipitation is *Mixed*.

(2-3) Assumption of precipitation particles

A precipitation particle is modeled as a spherical particle composed of liquid water, solid water, and air. The diameter of the spherical particle is drop seize D_b [mm] and the density of the spherical particle is ρ_b [g/cm^3].

The volume ratio of liquid water, solid water, and air to the particle is P_w, P_i, P_a, respectively. The following equation always holds.

$$P_w + P_i + P_a = 1 \tag{101}$$

The density of liquid water, solid water, and air is ρ_w, ρ_i, ρ_a, respectively. Then, the density of the particle can be given as below.

$$\rho_b = P_w\rho_w + P_i\rho_i + P_a\rho_a \tag{102}$$

Generally, we can assume ρ_w=1.0(g/cm^3). ρ_i is also constant (for example, ρ_i=0.92). Moreover, ρ_a can be regarded to be 0(g/cm^3) for simplicity. With these constant values, Eq. (102) can be simplified into (103).

$$\rho_b = P_w + 0.92P_i \tag{103}$$

(2-4) Setting of volume ratio and density

(2-4-1) Liquid phase particle

Obviously, P_w=1、P_i=P_a=0、ρ_b=1.0(g/cm^3).

(2-4-2) Mixed phase particle

First, P_w is set based on Awaka's model or TRMM/PR's experience. Then, ρ_b can be calculated by the following empirical equation.

$$\rho_b = \sqrt{P_w} \tag{104}$$

Then, P_i can be calculated by Eq. (102) with ρ_a=0.

$$P_i = (\rho_b - P_w\rho_w)/\rho_i \tag{105}$$

(2-4-3) Solid phase particle

First, ρ_b is set, for example, ρ_b=0.10(g/cm3). As P_w=0, P_i can be calculated by Eq. (105).

(2-5) Dielectric constants

ε_b is calculated by mixing rule, for example given in Eq. (106).

$$\frac{\varepsilon_b - 1}{\varepsilon_b + U} = P_w \frac{\varepsilon_w - 1}{\varepsilon_w + U} + P_i \frac{\varepsilon_i - 1}{\varepsilon_i + U} + P_a \frac{\varepsilon_a - 1}{\varepsilon_a + U} \tag{106}$$

where U is given as below,

$$U = 2.0 \qquad (\text{if } \rho_b \le 0.09\ \text{g/cm}^3), \tag{107a}$$

$$U = 2.0e^{13.0(\rho_b - 0.09)} \qquad (\text{if } \rho_b > 0.09\ \text{g/cm}^3). \tag{107b}$$

ε_w and ε_i are dielectric constants of water and ice and are functions of particle temperature, and ε_a is dielectric constants of air. As ε_a is approximated to 1, Eq. (106) can be simplified to Eq. (108).

$$\frac{\varepsilon_b - 1}{\varepsilon_b + U} = P_w \frac{\varepsilon_w - 1}{\varepsilon_w + U} + P_i \frac{\varepsilon_i - 1}{\varepsilon_i + U} \tag{108}$$

(2-6) Falling velocity

Falling velocity V_b of the particle can be given as below.

$$V_b = 3.3 \times [\rho_b - \rho_a]^{1/2} \qquad (\text{if } \rho_b \le 0.05\,\text{g/cm}^3) \tag{109a}$$

$$V_b = 8.8 \times [0.1 D_b (\rho_b - \rho_a)]^{1/2} \qquad (\text{if } 0.05\,\text{g/cm}^3 \le \rho_b \le 0.3\,\text{g/cm}^3) \tag{109b}$$

$$V_b = \frac{(\rho_b{}^{1/3} - 0.3^{1/3})}{(1.0 - 0.3^{1/3})}(V_R - V_{b0.3}) + V_{b0.3} \qquad (\text{if } 0.3\,\text{g/cm}^3 < \rho_b \le 1.0\,\text{g/cm}^3) \tag{109c}$$

where V_R is falling velocity when the particle is melted to rainfall, and is given as Eq. (110).

$$V_R = 4.854 \times D_m \times \exp(-0.195 D_m) \tag{110}$$

where D_m is a diameter after melting, and the relationship between D_b and D_m are as follows.

$$D_b = D_m \rho_b{}^{-1/3} \tag{111}$$

In Eq. (109c), $V_{b0.3}$ is the falling velocity calculated in Eq. (109b) with $\rho_b = 0.3\,\text{g/cm}^3$.

(2-7) Drop size distribution function

(2-7-1) Liquid phase

Gamma distribution function may be most commonly used for the drop size distribution function in liquid phase. The function is given as below.

$$N(D) = N_0 D^{\mu} \exp\left[-\frac{(3.67 + \mu)D}{D_0}\right], \tag{112}$$

where μ should be known. In Eq. (20), N^* corresponds to N_0, D^* corresponds to D_0, and n is given as Eq. (113).

$$n(D; D_0) = D^{\mu} \exp\left[-\frac{(3.67 + \mu)D}{D_0}\right] \tag{113}$$

(2-7-2) Mixed phase and solid phase

It is assumed that when all the particles are melted to liquid particles, the drop size distribution

obeys Eq. (112).With Eq. (111), Eq. (112) can be expressed by D_b and ρ_b.

$$N(D_b)dD_b = N_0 {\rho_b}^{(\mu+1)/3} {D_b}^{\mu} \exp\left[-\frac{(3.67+\mu)D_b\rho_b}{D_0}\right]dD_b \tag{114}$$

Eq. (114) can be modified to Eq. (115), if we consider the difference of number density caused by the difference of falling velocity as Non-break up and Non-coalescence model (N/N model) assumes.

$$N(D_b)dD_b = N_0 {\rho_b}^{(\mu+1)/3} {D_b}^{\mu} \frac{V_R(D_m)}{V_b(D_b)} \exp\left[-\frac{(3.67+\mu)D_b\rho_b}{D_0}\right]dD_b \tag{115}$$

(2-8) k-Z_e relation

The coefficients α and β of k-Z_e relation and the reliability of ε are set. Their values at the nodes are set first and those at other range bins are estimated by interpolation. In advanced procedure, for single-beam pixels in DF algorithm, k-Z_e relation can be set by referring the retrieval results in neighboring dual-beam pixels.

(3) DSD Look up table

k-Z_e relation are set by ground measurements (radar, disdrometer) and TRMM/PR experience for liquid phase. According to the N/N model, drop size distribution of liquid precipitation satisfying k-Z_e relation can be converted to that of melting or solid precipitation, then k-Z_e relationship can be approximated.

With actual measurement of DPR, DSD look up table should be modified and be dependent on land/ocean types, regions, and seasons. Furthermore, DSD look up table will be changed to DSD database, which can be updated regularly with the execution of the algorithm.

3.2.5 Surface Reference Technique Module

1. Objectives and functions of the algorithm

The primary purpose of the SRT is to compute the path-integrated attenuation (PIA) using the surface reference technique (SRT). The surface reference technique rests on the assumption that the difference between the measurements of the normalized surface cross section (in dB) within and outside the rain provides an estimate of the PIA.

For the DPR, the method is to be applied to the Ku-band as well as the Ka-band and Ka-band high sensitivity (Ka_HS) data. The basic set of output products for each of the channels (Ku, Ka and Ka_HS) will consist of a rain flag (from the Preparation Module), a PIA estimate (when rain is present) and an associated reliability. As in the TRMM algorithm 2a21, version 7, the primary output for each channel will be an effective or 'best' PIA estimate; in addition, however, PIA estimates corresponding to specific types of surface reference data will also be generated. These are described below. The standard PIA estimates will be produced by processing the data from the 3 channels (Ku, Ka, Ka_HS) independently. However, to account for the possibility of estimates generated by taking advantage of the dual-wavelength behavior of the surface cross sections, a dual-wavelength-derived PIA at Ku- and Ka-band will also be generated. These dual-wavelength estimates are discussed in section 8.

For each channel (Ku, Ka and Ka_HS), a spatially or temporally-averaged estimate of the rain-free normalized radar surface cross section (σ^0 or NRCS) is used as a reference value for computing the PIA. The algorithm computes up to five alternative estimates of PIA (corresponding to five different σ^0 reference estimates) for each of the three channels. An effective PIA is obtained by weighting the individual estimates by a factor that is inversely dependent on the variance of the estimate. Some of the reference estimates depend on the direction of processing, so the orbit is processed twice—in the forward direction, and again backward with respect to the orbital direction. This provides two reference values for the direction-sensitive methods. The reference estimates are described below:

Along-track Spatial Average: An average of the N_s most recent rain-free σ^0 measurements in same angle bin and with the same surface type (nominally, N_s=8). This estimate is referred to as the *spatial along-track average*. The reference data are computed by running the orbit both forward and backward. Such reference data are needed for the 49 angle bins at Ku-band as well as the 25 angle bins at Ka-band and the 24 angle bins at Ka-band HS for both forward and backward processing.

Hybrid: The hybrid reference data set results from a quadratic fit of the along-track spatial average data over the angles bins within the cross-track swath. This is explained below in more detail. For the Ku-band, separate fits are done for the inner (less than 11.25°) and outer swath (greater than 11.25°). As

with the along-track spatial reference, the cross-track hybrid is computed twice by processing the orbit forward and backward. For the Ka and Ka_HS channels, a single quadratic fit to the data over the swath should be sufficient.

Temporal Average: For Ku-band, this data set consists of monthly statistics (sample mean, sample mean square and number of data points) of rain-free σ^0 data at 0.1°×0.1° latitude-longitude cells, categorized into 26 incidence angles ±0.75° × j, j=0,..,24 where a 26th category is defined to account for incidence angles beyond 18°. Three 0.1°×0.1° files are computed for each month (for a total of thirty-six temporal reference files) for land, ocean and coastal backgrounds. Nominally, the temporal statistics from the TRMM Ku-band PR will be used for the Ku-band channel of the DPR. Shortly after launch, an analysis of σ^0(Ku) data from the DPR will be used to determine whether the TRMM reference data can be used for the DPR Ku-band channel.

For Ka-band, the temporal data set will be identical except that the number of angle bins required is 14 rather than 26. For the Ka-band high resolution temporal data set, 13 angle bins are required.

In addition to these data sets, another intermediate file will be needed to store cross products. A discussion on the proposed files and sizes of these intermediate files is given in section 5.

Forward-Backward Processing

Different estimates for along-track and hybrid methods are obtained from forward and backward processing. This provides up to five estimates—*Forward Along-track*, *Forward Hybrid*, *Backward Along-track*, *Backward Hybrid*, *and Temporal* - for each rain observation. Note that the hybrid estimates are only available over ocean since the cross-track fitting procedure does not work well over land. The different reference estimates are filtered according to various criteria. For example, an along-track estimate is dropped if the location of the reference data is too far from the observed rain point. A temporal estimate is dropped if the number of observations in the reference cell is too low. Details are given in sections 12 and 13. The surviving estimates are weighted by the inverse of their associated variance. The weighted estimates are combined to yield an effective PIA for each of the channels, (`pathAtten_Ku, pathAtten_Ka, pathAtten_KaHS`). The individual estimates, (`PIAalt_Ku, PIAalt_Ka, PIAalt_KaHS`), and their weights, (`PIAweight_Ku, PIAweight_Ka, PIAweight_KaHS`) will be included in the product. A discussion of the weights and the effective PIA, variance, and reliability factor is given in section 11.

In addition to the sample mean of the NRCS as a function of angle bin (and in some cases location or surface type), the reference data sets also include the standard deviation of the

data used to compute the sample mean. This quantity is used to estimate the stability of the reference rain-free mean NRCS.

In the spatial (along-track) surface reference data set, the mean and standard deviation of the NRCS are calculated over a running window of N_s fields of view before rain is encountered (currently, N_s=8). These operations will be performed separately for each of the 49+2 incidence angles for the Ku-band channel of the DPR, corresponding to the cross-track scan from -18° to +18° with respect to nadir. The 2 additional angle bins (making the total 51 rather than 49) are used to take care of non-zero pitch/roll angles that can shift the incidence angle outside the normal range. Note that the zenith angle increment is taken to be 0.75° so that the angle bins can be defined by ±0.75° × j, j=0,..,24. The Ka- and Ka_HS channels will be treated in the same way. The difference is that 25+2 angle bins will be needed for the Ka-band and 24+2 for the Ka_HS channel.

Basic Processing

When rain is encountered, the means and standard deviations of the reference σ^0 values are retrieved from the along-track spatial (forward and backward), the hybrid (forward and backward) and temporal surface reference data sets. If a valid surface reference data set exists for one of the above estimates, then, denoting this by the jth estimate, the 2-way path attenuation (PIA) is computed from the equation:

$$PIA_j = \left\langle \sigma^0_{NR} \right\rangle_j - \sigma^0$$

where $<\sigma^0_{NR}>_j$ is the jth reference estimate and σ^0 is the value of the apparent normalized radar surface cross section at the rain field of view of interest.

To obtain information as to the reliability of the jth PIA estimate we consider the ratio of the PIA, as derived in the above equation, to the standard deviation as calculated from the rain-free σ^0 values and stored in the reference data set. Labeling this as $\texttt{std\_dev}_j$(reference value), then the reliability factor of the jth PIA estimate is defined as:

$$\text{reliabFactor}_j = \frac{\text{PIA}_j}{\text{std\_dev}_j(\text{reference value})}$$

When this quantity is large, the reliability is considered high and conversely.

The effective PIA, PIA_{eff}, and the corresponding reliability factor can be expressed in similar ways. From section 10, we have:

$$PIA_{eff} = (\Sigma u_j)^{-1} \Sigma u_j PIA_j$$
$$\text{Rel}_{eff} = (\Sigma u_j)^{-1/2} \Sigma u_j PIA_j$$

Where u_j is the inverse of the variance, σ_j^2, associated with the jth reference data set:

$$u_j = 1/\sigma_j^2$$

Note that the summations are assumed to range over all valid reference data sets, even if the PIA's are negative. Over land, there can be a maximum of 3 valid reference data sets (forward and backward along-track and temporal) while over ocean there can be as many as five since the forward/backward hybrid reference data sets may be valid as well. Note finally, that in the notation used above:

$$\sigma_j = std\_dev_j(reference\_value)$$

3. Input Variables

`sigmaZero_Ku(49)` [real*4]

Normalized backscattering radar cross section of the surface (dB) (NRCS) at Ku-band for the 49 angles bins in the radar scan (unitless). From the Preparation Module, naming convention TBD.

`rainFlag_Ku(49)` [integer*2] rain/no-rain flag from Preparation Module, naming convention TBD.

`sigmaZero_Ka(25)` [real*4]

Normalized backscattering radar cross section of the surface (dB) (NRCS) at Ku-band for the 49 angles bins in the radar scan (unitless). From the Preparation Module.

`rainFlag_Ka(25)` [integer*2] rain/no-rain flag from Preparation Module.

`sigmaZero_KaHS(24)` [real*4]

Normalized backscattering radar cross section of the surface (dB) (NRCS) at Ku-band for the 49 angles bins in the radar scan (unitless). From the Preparation Module.

`rainFlag_KaHS(24)` [integer*2] rain/no-rain flag from Preparation Module.

4. Definitions of Output Variables

4a. Ku-band variables:

pathAtten_Ku(49) [real*4]

Estimated 2-way path-attenuation in (dB) at Ku-band where

$$\text{pathAtten} = 2\int_0^{r_s} k(s)ds$$

where *k*(s) is the attenuation coefficient in dB/km and integral runs from storm top to the surface. The path attenuation is often designated as the PIA, the path-integrated attenuation.

In the notation used above and in section 10:

$$pathATTen = PIA_{eff} = (\Sigma u_j)^{-1}\Sigma u_j PIA_j$$

where

$$u_j = 1/\sigma_j^2$$

PIAalt_Ku(5,49) [real*4]

The path-integrated attenuation from the jth estimate, where

PIAalt_Ku(j=1, k)= PIA_Ku from forward along-track spatial at kth angle bin

PIAalt_Ku (j=2, k)= PIA_Ku from forward hybrid at kth angle bin

PIAalt_Ku (j=3, k)= PIA_Ku from backward along-track spatial at kth angle bin

PIAalt_Ku (j=4, k)= PIA_Ku from backward hybrid at kth angle bin

PIAalt_Ku (j=5, k)= PIA_Ku from temporal at kth angle bin

PIAweight_Ku(5,49) [real*4]

The weights of the individual PIA_Ku estimates used in deriving the effective PIA_Ku. The sum of the weights should equal one.

$$w_j = \frac{1}{\sigma_j^2}\frac{1}{\Sigma\frac{1}{\sigma_j^2}} \equiv u_j / \Sigma u_j$$

where

$$u_j = 1/\sigma_j^2$$

$$\sum w_j = 1$$

reliabFlag_Ku(49) [integer*2]

Reliability Flag for the PIA_{eff}(Ku) estimate,

= 1 (PIA_{eff} estimate is reliable) - see definitions below

= 2 (is marginally reliable)

= 3 (is unreliable)

= 4 (provides a lower bound to the path-attenuation)

= 9 (no-rain case)

`reliabFactor_Ku(49)` [real*4]

Reliability Factor for the effective PIA_Ku estimate, `pathAtten_Ku. This is` defined as:

$$reliabFactor = \mathrm{Rel}_{eff} = (\Sigma u_j)^{-1/2} \Sigma u_j PIA_j$$

`RFactorAlt_Ku(5,49)` [real*4]

The reliability factors associated with the individual PIA estimates.

$$RFactorAlt_j = \mathrm{Rel}_j = PIA_j / \sigma_j ;\ j = 1,...,5$$

`rainFlag_Ku(49)` [integer*2]

Rain/no-rain flag (rain=1; no-rain=0). If the Preparation module rain flag includes a rain possible flag, this will be included here in the no-rain category; only the rain-certain category will be considered rain.

`incAngle_Ku(49)` [real*4]

Incidence angle with respect to nadir (in degrees); pitch/roll correction is included. (Obtained from the Preparation Module.)

`refScanID_Ku(2,2,49)` [integer*2]

`refScanID` gives the number of scan lines between the current scan and the beginning (or end) of the along-track reference data at each angle bin. The values are computed by the equation: `Current Scan Number - Reference Scan Number`. The values are positive for the Forward estimates and negative for the Backward estimates. The Fortran indices are:

1,1 - Forward - Near reference

2,1 - Forward - Far reference

1,2 - Backward - Near reference

2,2 - Backward - Far reference

`surfaceTracker_Ku(49)` [integer*2] - may be obsolete

= 1 (surface tracker locked - central angle bin)

= 2 (unlocked - central angle bin)

= 3 (peak surface return at normally-sampled gate - outside central swath)

= 4 (not at normally-sampled gate - outside central swath)

surfTypeFlag_Ku(49) [integer*2]

= 0 (ocean)

= 1 (land)

= 2 (coast)

= 3 (unknown or of a category other than those above or 'mixed' type)

4b. Ka-band variables:

pathAtten_Ka(25) [real*4]

Estimated 2-way Ka-band path-attenuation in (dB) where

$$\text{pathAtten} = 2\int_0^{r_s} k(s)ds$$

where $k(s)$ is the attenuation coefficient in dB/km at Ka-band and integral runs from storm top to the surface. The path attenuation is often designated as the PIA, the path-integrated attenuation.

In the notation used above and in section 10:

$$pathATTen = PIA_{eff} = (\Sigma u_j)^{-1}\Sigma u_j PIA_j$$

where

$$u_j = 1/\sigma_j^2$$

PIAalt_Ka(5,25) [real*4]

The path-integrated attenuation from the jth estimate, where

PIAalt_Ka(j=1, k)= PIA from forward along-track spatial at kth angle bin

PIAalt_Ka (j=2, k)= PIA from forward hybrid at kth angle bin

PIAalt_Ka (j=3, k)= PIA from backward along-track spatial at kth angle bin

PIAalt_Ka (j=4, k)= PIA from backward hybrid at kth angle bin

PIAalt_Ka (j=5, k)= PIA from temporal at kth angle bin

PIAweight_Ka(5,25) [real*4]

The weights of the individual PIA estimates used in deriving the effective PIA. The sum of the weights should equal one.

$$w_j = \frac{1}{\sigma_j^2}\frac{1}{\Sigma\frac{1}{\sigma_j^2}} \equiv u_j / \Sigma u_j$$

where

$u_j = 1/\sigma_j^2$

$\sum w_j = 1$

reliabFlag_Ka(25) [integer*2]

Reliability Flag for the PIA_{eff}(Ka) estimate,

= 1 (PIA_{eff} estimate is reliable) - see definitions below

= 2 (is marginally reliable)

= 3 (is unreliable)

= 4 (provides a lower bound to the path-attenuation)

= 9 (no-rain case)

reliabFactor_Ka(25) [real*4]

Reliability Factor for the effective Ka-band PIA estimate, `pathAtten_Ka. This is` defined as:

$$reliabFactor = \mathrm{Rel}_{eff} = (\Sigma u_j)^{-1/2}\Sigma u_j PIA_j$$

RFactorAlt_Ka(5,25) [real*4]

The reliability factors associated with the individual PIA estimates.

$$RFactorAlt_j = \mathrm{Rel}_j = PIA_j / \sigma_j;\ j = 1,...,5$$

rainFlag_Ka(25) [integer*2]

Rain/no-rain flag (rain=1; no-rain=0). This will be obtained from the Preparation Module.

incAngle_Ka(25) [real*4]

Incidence angle with respect to nadir (in degrees); pitch/roll correction is included. This quantity will be obtained from the Preparation Module.

refScanID_Ka(2,2,25) [integer*2]

`refScanID` gives the number of scan lines between the current scan and the beginning (or end) of the along-track reference data at each angle bin. The values are computed by the equation: `Current Scan Number - Reference Scan Number`. The values are positive for the Forward estimates and negative for the Backward estimates. The Fortran indices are:

1,1 - Forward - Near reference

2,1 - Forward - Far reference

1,2 - Backward - Near reference

2,2 - Backward - Far reference

`surfaceTracker_Ka(25)` [integer*2] - may be obsolete

= 1 (surface tracker locked - central angle bin)

= 2 (unlocked - central angle bin)

= 3 (peak surface return at normally-sampled gate - outside central swath)

= 4 (not at normally-sampled gate - outside central swath)

`surfTypeFlag_Ka(25)` [integer*2]

`= 0 (ocean)`

`= 1 (land)`

`= 2 (coast)`

`= 3 (unknown or of a category other than those above or ‘mixed’ type)`

4c. KaHS-band variables:

`pathAtten_KaHS(24)` [real*4]

Estimated 2-way Ka-band high sensitivity path-attenuation in (dB) where

$$\text{pathAtten} = 2\int_0^r k(s)ds$$

where *k*(s) is the attenuation coefficient in dB/km and integral runs from storm top to the surface. The path attenuation is often designated as the PIA, the path-integrated attenuation.

In the notation used above and in section 10:

$$pathATTen = PIA_{eff} = (\Sigma u_j)^{-1}\Sigma u_j PIA_j$$

where

$$u_j = 1/\sigma_j^2$$

`PIAalt_KaHS(5,24)` [real*4]

The path-integrated Ka_HS attenuation from the jth estimate, where

PIAalt_KaHS(j=1, k)= PIA from forward along-track spatial at kth angle bin

PIAalt_KaHS(j=2, k)= PIA from forward hybrid at kth angle bin

PIAalt_KaHS(j=3, k)= PIA from backward along-track spatial at kth angle bin

PIAalt_KaHS(j=4, k)= PIA from backward hybrid at kth angle bin

PIAalt_KaHS(j=5, k)= PIA from temporal at kth angle bin

`PIAweight_KaHS(5,24)` [real*4]

The weights of the individual KaHS PIA estimates used in deriving the effective PIA. The sum of the weights should equal one.

$$w_j = \frac{1}{\sigma_j^2}\frac{1}{\Sigma\frac{1}{\sigma_j^2}} \equiv u_j / \Sigma u_j$$

where

$$u_j = 1/\sigma_j^2$$

$$\sum w_j = 1$$

`reliabFlag_KaHS(24)` [integer*2]

Reliability Flag for the KaHS PIA_{eff} estimate,

= 1 (PIA_{eff} estimate is reliable) - see definitions below

= 2 (is marginally reliable)

= 3 (is unreliable)

= 4 (provides a lower bound to the path-attenuation)

= 9 (no-rain case)

`reliabFactor_KaHS(24)` [real*4]

Reliability Factor for the KaHS effective PIA estimate, `pathAtten_KaHS. This is` defined as:

$$reliabFactor = \mathrm{Rel}_{eff} = (\Sigma u_j)^{-1/2} \Sigma u_j PIA_j$$

`RFactorAlt_KaHS(5,24)` [real*4]

The reliability factors associated with the individual PIA estimates.

$$RFactorAlt_j = \mathrm{Rel}_j = PIA_j / \sigma_j ; \; j = 1,...,5$$

`rainFlag_KaHS(24)` [integer*2]

Rain/no-rain flag (rain=1; no-rain=0) The rain possible category from 1B-21 is included in the no-rain category; only the rain-certain category is considered rain.

`incAngle_KaHS(24)` [real*4]

Incidence angle with respect to nadir (in degrees); pitch/roll correction is included.

`refScanID_KaHS(2,2,24)` [integer*2]

`refScanID_KaHS` gives the number of scan lines between the current scan and the beginning (or end) of the along-track KaHS reference data at each angle bin. The values are computed by the equation: `Current Scan Number - Reference Scan Number`. The values are positive for the Forward estimates and negative for the Backward estimates. The Fortran indices are:

1,1 - Forward - Near reference

2,1 - Forward - Far reference

1,2 - Backward - Near reference

2,2 - Backward - Far reference

`surfaceTracker_KaHS(24)` [integer*2] - may be obsolete

= 1 (surface tracker locked - central angle bin)

= 2 (unlocked - central angle bin)

= 3 (peak surface return at normally-sampled gate - outside central swath)

= 4 (not at normally-sampled gate - outside central swath)

surfTypeFlag_KaHS(24) [integer*2]

= 0 (ocean)

= 1 (land)

= 2 (coast)

= 3 (unknown or of a category other than those above or 'mixed' type)

4d. Dual-wavelength derived PIA's:

The variables below are based on dual-wavelength processing of the data. A discussion of this is given in section 8.

pathAttenDW_Ku(25) [real*4]

Estimated 2-way Ku-band path-attenuation in (dB) where

reliabFactorDW_Ku(25) [real*4]

Reliability Factor for the PIA estimate, pathAttenDW_Ku.

pathAttenDW_Ka(25) [real*4]

Estimated 2-way Ka-band path-attenuation in (dB) where

reliabFactorDW_Ka(25) [real*4]

Reliability Factor for the PIA estimate, pathAttenDW_Ku.

4e. Other potential variables

Dr. Seto of Tokyo University has proposed a light-rain temporal surface reference data set. Whether additional PIA's and associated variables should be defined when the light-rain reference is used is to be determined. At minimum, a flag will be required to indicate that the light-rain reference has been used rather than the standard no-rain reference.

A less likely possibility is the use of an ocean-wind speed model or a land surface model that would provide alternate estimates of the PIA. One possibility of accommodating these, as well as the light-rain reference results, would be to increase the index on the PIAalt_Ku, PIAalt_Ka, PIAalt_KaHS and related variables. For example, if a separate PIA estimate is derived from the light-rain reference, the dimensions of PIAalt_Ku could be changed from (5, 49) to (6, 49). Similar changes could be made to the other variables.

5. Intermediate Files

To plan for the possible reuse of the TRMM PR-Ku intermediate files, we propose an extension of these files from the present latitude range of 37^0 S-37^0N to the GPM DPR latitude range of 67^0S-67^0N. Since the TRMM PR grid is 0.1^0x0.1^0 with 26 angle bins, then the proposed intermediate files for Ku-band DPR are:

Ku(3600, 1340, 26, 3) real*4 [1.5 GB] – ocean Ku reference data

Where the first index denotes longitude, the second latitude, the third angle bin and the fourth the statistic (sample mean, sample mean square, number of counts). It might be possible to condense these 3 files into a single file because of the small amount of overlap – i.e., for almost all cells in the grid, only one file will have non-zero count values.

For Ka-band, the requirement is almost identical except that 14, not 26, angle bins are needed:

Ka(3600, 1340, 14, 3) [real*4] [0.75 GB] –Ka reference data

For Ka_HS, 13 angle bins are needed:

KaHS(3600, 1340, 13, 3) [real*4] [0.75 GB] –KaHS reference data

Another set of intermediate files are needed to store the cross-product sigma-zero data. If the common Ku/Ka-band data have a single rain/no-rain designation, then the final index of these files can be 1, to store the sample mean of the cross-product: $\sigma^0_{NR}(Ku)*\sigma^0_{NR}(Ka)$, where NR stands for 'no-rain'. On the other hand, if the rain designations for the Ku- and Ka-band data are independent, then the final index of these files will be 6 in order to store the mean and mean square of the Ku- and Ka-band data as well as the number of counts for which both channels are designated as no-rain. The following assumes that only 1

dimension is needed so that this index can be omitted:

X(3600, 1340, 13) [real*4] [0.75 GB] –Ku/Ka cross product reference data

As in the 2a21 v7 algorithm, the intermediate files will be produced off-line and for each month. This circumvents the need to update the temporal files during operational processing.

A final consideration for the temporal files is light-rain reference data files proposed by Dr. Seto. The spatial resolution of these files and the conditions under which the data are to be stored have yet to be determined. Whether new PIA's fields should be defined or only a new flag, to indicate that the light-rain reference has been used for the PIA, is also at issue.

6. Description of the Processing Procedure

As in 2a21 v7, we propose that the full granule be first read in and stored. After this, each channel (Ku, Ka and KaHS) is to be processed twice, in the forward orbit sequence, and then backwards. This is done because the along-track and hybrid methods use rain-free reference observations from rain-free areas close to the rain. By processing the orbit backwards, we get independent reference estimates. This gives up to 5 estimates that can be combined or filtered to select a "best" estimate. The five estimates are *Forward Along-track*, *Forward Hybrid* (Ocean only), *Backward Along-track*, *Backward Hybrid* (Ocean only), and *Temporal*.

Although the standard estimates for the 3 channels can be done independently in this way, to allow for the possibility of dual-wavelength (or combined) processing of the data, a modification to the above procedure will be needed. Perhaps the easiest way of generalizing the processing is to add calculations of the $\sigma^0_{NR}(Ku)*\sigma^0_{NR}(Ka)$ *and* $\sigma^0_{R}(Ku)*\sigma^0_{R}(Ka)$during the Ka-band processing segment. This should allow estimates of Ku- and Ka-band PIAs from most of the methods that are being considered. See section 8 for details.

7. Interfaces to other algorithms:

All input data for this algorithm is from the Preparation Module; the outputs will be used by Solver Module and others (??).

8. Dual-wavelength Derived PIA Estimates

Data on $\sigma^0_{NR}(Ku)$ *and* $\sigma^0_{NR}(Ka)$ from the JPL APR2 airborne dual-wavelength radar suggests that the correlation of these quantities (i.e., the NRCS at Ku and Ka-band under rain-free conditions) can be quite high (0.99) over ocean at off-nadir angles. For near-nadir incidence angles over ocean the correlation decreases to about 0.8 while the data base over land is too sparse to make a determination regarding the correlation. In addition, if we consider the ratio $k(\lambda_2)/k(\lambda_1)$ where λ_2 is the wavelength of the Ka-band radar and λ_1 the wavelength at Ku-band we find that this is relatively constant for Rayleigh scattering, the only source of variability being the temperature dependence of the imaginary part of the dielectric factor, which is directly proportional to k. The variability of this quantity also increases when the scatterers are no longer Rayleigh. Nevertheless, there is reason to suppose that a fair or good a priori estimate of $k(\lambda_2)/k(\lambda_1)$, and therefore of $A(\lambda_2)/A(\lambda_1)$, can be obtained, where $A(\lambda)$ is the 2-way path attenuation at λ.

We assume that the rain-free data ($\sigma^0_{NR}(\lambda_1=Ku)$, $\sigma^0_{NR}(\lambda_2=Ka)$) are well correlated and that the regression line is given by:

$$\sigma^0(\lambda_2) = \alpha + \beta\sigma^0(\lambda_1)$$

Assume that a measurement in rain is made with the measured or apparent NRCS data given by: $\{\sigma^0_m(\lambda_1), \sigma^0_m(\lambda_2)\}$. Assume further that the means of the reference data are given by $\{\langle\sigma^0(\lambda_1)\rangle, \langle\sigma^0(\lambda_2)\rangle\}$.

For the standard, single wavelength application of the SRT, the path attenuations would be given by:

$$A(\lambda_i) = \langle\sigma^0(\lambda_i)\rangle - \sigma^0_m(\lambda_i); \quad i=1,2$$

These quantities are shown in the diagram below. However, we can find a new reference data point $\{\sigma^0_{ref}(\lambda_1), \sigma^0_{ref}(\lambda_2)\}$ as that point along the regression line for which $A(\lambda_2)/A(\lambda_1)$ is some constant, say γ. With these conditions, the reference data point is found to be:

$$\sigma^0_{ref}(\lambda_1) = (\gamma-\beta)^{-1}[(\gamma\sigma^0_m(\lambda_1) - \sigma^0_m(\lambda_2)) + (\langle\sigma^0(\lambda_2)\rangle - \beta\langle\sigma^0(\lambda_1)\rangle)]$$

$$\sigma^0_{ref}(\lambda_2) = \gamma\beta(\gamma-\beta)^{-1}[(\sigma^0_m(\lambda_1) - \gamma^{-1}\sigma^0_m(\lambda_2)) - (\langle\sigma^0(\lambda_1)\rangle - \beta^{-1}\langle\sigma^0(\lambda_2)\rangle)]$$

Where, as shown in the diagram, the modified PIAs are given by

$$A'(\lambda_i) = \sigma^0_{ref}(\lambda_i) - \sigma^0_m(\lambda_i); \; i=1,2$$

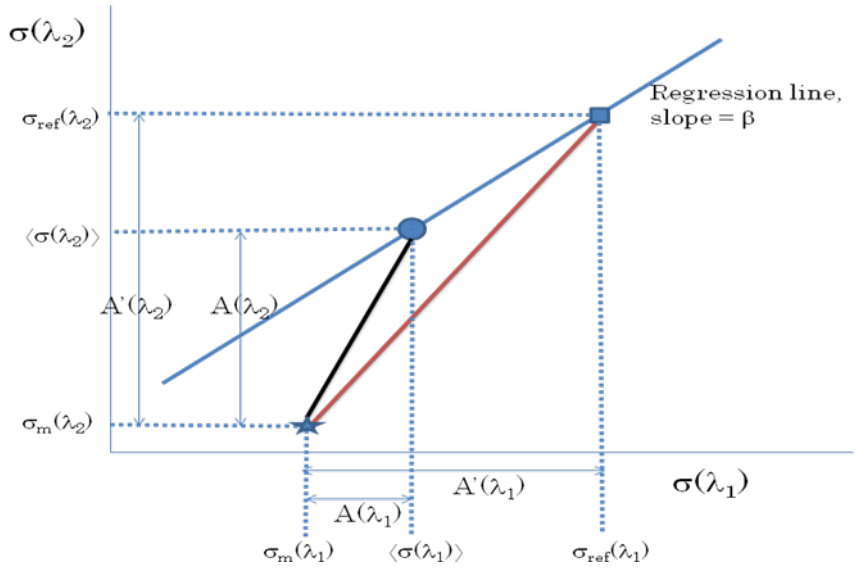

Fig. Schematic diagram of path attenuation estimates from dual-wavelength surface cross section data.

9. The Cross-track Hybrid Surface Reference Method (to be revised)

A quadratic fit of the spatial along-track reference data provides a reference curve from which the path attenuation can be estimated. As noted earlier, the spatial along-track average at each angle bin is computed from the last N_s (=8) rain-free observations over the same background type (i.e., ocean, land, or coast). The standard deviation from the spatial average is used as a weight in the fitting procedure. The fitted function is a quadratic where the fitting routine is based on the `LFIT` routine from Numerical Recipes (Press, et. al., 1989).

The spatial average at the ith angle bin is the average of the last N_s rain-free surface reflectivity values, σ^0_{NR},

$$y_i = \left\langle \sigma^0_{\mathrm{NR}}(\theta_i) \right\rangle$$

Using "AS" to denote the along-track spatial reference, the standard deviation is

$$S_{\mathrm{AS}}(\theta_i) = \sqrt{\mathrm{var}(\sigma^0_{\mathrm{NR}}(\theta_i))}$$

The fit function is the quadratic

$$\mathrm{yfit}(\theta_i) = a + b\theta_i + c\theta_i^2$$

We determine the parameters a, b, and c by minimizing

$$\chi^2 = \sum_{i=1}^{49} \left(\frac{y_i - \mathrm{yfit}(\theta_i)}{S_{\mathrm{AS}}(\theta_i)} \right)^2$$

The (2-way) hybrid PIA is the difference between the Surface Reference value, $\mathtt{yfit}(\theta_i)$, and the apparent (attenuated) surface cross section, σ^0_i:

$$A_i = \text{yfit}(\theta_i) - \sigma_i^0$$

There are several reliability factors that can be defined for this estimate. Nominally, we take this to be the following:

$$\text{reliabFactor\_3}(i) = \frac{A_i}{\text{rms}(S_{\text{AS}})}$$

Where

$$\text{rms}(S_{\text{AS}}) = \sqrt{\frac{1}{N_x}\sum_{j=1}^{Nx} S_{\text{AS}}^2(\theta_j)}$$

where N_x is the number of fields of view in the scan. For Ku-band N_x=49, for Ka-band, N_x=25 and for KaHS-band, N_x=24.

10. Revised Angle Bin Definitions (to be revised)

The SRT algorithm defines two angle bins. The first, angle1, is computed from the absolute value of the incidence angle, and is used to categorize observations for the temporal Surface Reference Technique (SRT). It ranges from 1 to 26 for Ku-band (Fortran array convention). The other angle bin, angle2, depends on the signed incidence angle, and is used for the spatial SRT. It ranges from 1 to 51 for Ku-band.

The angle bins angle1 and angle2 are defined such that

$$(\text{angle1} - 1 - 0.5)\Delta\theta \le |\theta| < (\text{angle1} - 1 + 0.5)\Delta\theta$$
$$(\text{angle2} - 26 - 0.5)\Delta\theta \le \theta < (\text{angle2} - 1 + 0.5)\Delta\theta$$

where θ is the incidence angle and $\Delta\theta$ is the angle bin size.

These relations can be expressed more simply by

$$\text{angle1} = \text{int}\left(\frac{|\theta|}{\Delta\theta} + 1 + 0.5\right)$$

$$\text{angle2} = \text{int}\left(\frac{\theta}{\Delta\theta} + 26 + 0.5\right)$$

respectively.

The nominal choice of $\Delta\theta$ is a constant value of 0.75°.

11. Definitions of the Effective PIA, Variance and Reliability Factor

In the SRT for the DPR, for each channel (Ku, Ka and KaHS) multiple estimates of PIA are generated. These correspond to different surface reference estimates – i.e., the estimate of the rain-free NRCS or

σ°_{NR}. Specifically, we have the following situation

$$PIA_j = \left\langle \sigma^0_{NR} \right\rangle_j - \sigma^0 \tag{1}$$

where the first term on the right-hand side is the jth surface reference value and the second term is the apparent NRCS in rain. Note that there are as many as five reference values, corresponding to forward along-track, forward hybrid (cross-track), backward along-track, backward hybrid (cross-track) and temporal. Over land and coast, however, only three are used since the hybrid approach is not reliable. Associated with the jth reference data set is a variance, σ_j^2:

$$\mathrm{var}(PIA_j) = \mathrm{var}[\left\langle \sigma^0_{NR} \right\rangle_j] = \sigma_j^2 \tag{2}$$

From these PIA estimates we want to obtain an effective PIA. We assume it can be written in the form:

$$PIA_{eff} = \Sigma w_j PIA_j \tag{3}$$

Where the weights, w_j, are such that

$$\Sigma w_j = 1 \tag{4}$$

We assume that the individual PIA estimates are statistically independent so that the variance of PIA_{eff} is:

$$\mathrm{var}(PIA_{eff}) = \Sigma w_j^2 \sigma_j^2 \tag{5}$$

To minimize this, subject to the side condition given by (4), we use the method of Lagrange multipliers where the expression

$$\Sigma w_j^2 \sigma_j^2 + \lambda(\Sigma w_j - 1) \tag{6}$$

is minimized with respect to the weights, w_j. Taking the partial derivatives of (6) with respect to w_i, then

$$2w_i\sigma_i^2 + \lambda = 0 \Rightarrow w_i = -\lambda / 2\sigma_i^2 \tag{7}$$

Also, using (4) gives

$$\Sigma w_j = -(\lambda/2)\Sigma(1/\sigma_j^2) = 1 \Rightarrow \lambda = -2/\Sigma(1/\sigma_j^2) \tag{8}$$

Substituting (8) into (7) gives an expression for the weights:

$$w_j = \frac{1}{\sigma_j^2}\frac{1}{\Sigma\frac{1}{\sigma_j^2}} \equiv u_j / \Sigma u_j \tag{9}$$

Where

$$u_j = 1/\sigma_j^2 \tag{10}$$

The effective PIA is then

$$PIA_{eff} = (\Sigma u_j)^{-1} \Sigma u_j PIA_j \tag{11}$$

If we define the reliability factor, Rel, as the ratio of the PIA to the standard deviation of the reference estimate, then for the jth reference estimate, we can write:

$$\mathrm{Rel}_j = PIA_j / \sigma_j \quad (12)$$

To apply this definition to the present situation, we define Rel_{eff} by the equation:

$$PIA_{eff} = (\Sigma u_j)^{-1} \Sigma u_j PIA_j \equiv \sigma_{eff} \mathrm{Rel}_{eff} \quad (13)$$

Computing Rel_{eff} requires a value for the standard deviation of the effective PIA. This can be found by substituting (9) into (5) and by noting that $\sigma_{eff}^2 = \mathrm{var}(PIA_{eff})$. This gives

$$1/\sigma_{eff}^2 = \Sigma(1/\sigma_j^2) \Rightarrow \sigma_{eff}^2 = (\Sigma(1/\sigma_j^2))^{-1} = (\Sigma u_j)^{-1} \quad (14)$$

Using (14) in (13) gives

$$\mathrm{Rel}_{eff} = (\Sigma u_j)^{-1/2} \Sigma u_j PIA_j \quad (15)$$

Equations (9), (11) and (15) define, respectively, the weights, effective PIA, and effective reliability factor as will be computed in the algorithm.

There are several issues related to these equations. For example, what should be done if none of the reference data sets exist? This situation can occur for measurements over small islands or small bodies of water or at coastal fields of view. For example, over a small island, there may be an insufficient number of non-raining fields of view adjacent to the rain area to form a valid spatial reference. In most cases, the temporal reference data set would be used (j=1 in the above equations) and the other reference estimates would be discarded. However, in some cases, there may be an insufficient number of data points in the temporal file to provide a valid estimate. In this case, a flag is set indicating that no valid reference data are available and all the output variables are set to -999. (Definitions of valid spatial and temporal reference data sets are discussed in sections 11 and 12 below.)

A somewhat different situation occurs if some of the reference data sets exist but all yield a negative PIA. For these cases, the individual variances will exist so that Rel_{eff}, PIA_{eff} and the effective variance should all exist. Note that for these cases Rel_{eff}, PIA_{eff} will be negative but the effective variance will be positive, as it should be.

A third type of situation occurs if one or more of the PIA estimates are positive and one or more of the PIA estimates are negative. In this case, the negative PIAs will be included in the definition of PIA_{eff}. In general, as long as the reference data is considered to be valid, the PIA will be used even if the value is negative.

According to these scenarios, there will be only one type of raining situation where the output variables will need to be set to some default value and this occurs when none of the reference data sets exist or are valid. This is expected to be a very small fraction relative to the total number of rain cases.

12. Excluding Spatial Reference Data based on the refScanID Variable

This section relates to determining the circumstances under which we assume a spatial reference estimate to be valid. For the forward-going spatial reference, reference data will almost always exist. An exception is if rain is encountered at the beginning of the orbit before N_s(=8) rain-free fields of view have been measured at a particular incidence angle. A similar exception occurs for the backward spatial methods: this occurs, however, at the end of the orbit rather than the beginning. In all other cases, forward and backward spatial reference data should exist. The question is how should we exclude spatial reference estimates if the data are taken at locations far from the raining area. To make this definite we intend to implement the following rules in the algorithm.

See definition of refScanID_Ku(2,2,49) in section 4.

The forward along-track spatial reference will be assumed to be invalid (at angle bin j) if:
|refScanID_Ku(2,1,j)| > 50.

Similarly, the backward along-track spatial reference will be assumed to be invalid (at angle bin j) if:
|refScanID_Ku(2,2,j)| > 50.

The above conditions are equivalent to stating that, for a particular incidence angle, all the spatial reference data must be taken within 50 scans of the scan at which rain is encountered.

The criteria for the hybrid cross-track are more complicated because two quadratic fits are used for the inner and outer portion of the swath. Nominally, we will assume that if there are 15 or more angle bins in the inner portion of the swath for which:

$$|\text{refScanID\_Ku}(2,1,j)| \leq 50$$

then the forward hybrid cross-track method will be applied.

Similarly in the outer portion of the swath, if there are 15 or more angle bins in this portion of the swath for which:

$$|\text{refScanID\_Ku}(2,1,j)| \leq 50$$

then the forward hybrid cross-track method will be applied.

Application of the backward hybrid cross-track will follow the same rule, based on refScanID_Ku(2,2,j). For the Ka and KaHS channels, similar definitions for the quantities refScanID_Ka and refScanID_KaHS will be used.

13. Issues Concerning Temporal Reference Data

Under raining conditions, the temporal data file that is accessed depends on the month and surface type under which the raining measurement is made. The reference data at the 0.1°×0.1° cell and angle-bin of interest consists of the mean, mean square and number of rain-free data points, N_t. The reference data will be considered valid if $N_t > N_{thres}$ where nominally, N_{thres} =10; otherwise, the temporal reference data are considered invalid and not to be used in the calculation of the effective PIA.

The high resolution grid (0.1°×0.1°) proposed for the DPR reference data implies that it will take a number of years to populate this. (This can be shown to be the case by computing the number of grid points of the temporal files relative to the volume of output data as a function of time after launch.) An exception to this is the Ku-band data from 37S-37N: if the 12+ years of TRMM PR data can be used, then a large amount of high resolution data will be available in the region. Outside this 37S-37 N area and for all the Ka, KaHS data, the high resolution grid will be poorly populated even after several years. One way to mitigate this problem is to use a flexible averaging grid. For example, a temporal reference estimate can be formed about a particular latitude/longitude by taking the (0.1°×0.1°) reference data about this point to as large an area as desired – or until a sufficient number of reference data points are found. The impact on the CPU and I/O of this 'up-scaling' procedure will require testing.

3.2.6 Solver module

(1) Objective

The primary objective of Solver module is to retrieve drop size distribution and calculate some physical variables.

(2) Processes at single-beam pixels

(2-1) Target pixels and range bins

Pixels with precipitation and without any errors are processed. Estimation of physical variables is done for range bins from the storm top range bin to the land surface range bin. The “echo region” means continuous range bins with precipitation starting at the storm top range bin. Below the echo region, “noise region” usually exists down to the land surface. The lowest range bin in echo region is called echo bottom range bin. The echo bottom range bin is the same with or above the clutter free bottom range bin. Echo bottom range bin is higher than clutter free bottom range bin when there is strong attenuation. When one or few no-precipitation range bins are intervened by continuous precipitation range bins, it is worth trying to interpolate Z_m at the no-precipitation range bins so that echo region is extended.

(2-2) Retrieval

As the TRMM/PR standard algorithm, a hybrid use of HB method and SRT is planned.

For echo region, attenuation correction can be done by Eq. (40) with the default parameters of α and β. Then, Z_e is extrapolated to the noise region. Most simply, it is assumed that Z_e in noise region is constant and is the same with that in the echo bottom range bin. More sophisticated extrapolation method, which is dependent on the precipitation type, should be considered in near future.

For noise region, k can be calculated from k-Z_e relation, and Z_m can be calculated by half-range-bin approximation. Then, ζ defined in Eq. (201) can be calculated.

$$\zeta = 0.2(\ln 10)\beta \int_0^{r_s} \alpha(s) Z_m(s)^{\beta} ds \tag{201}$$

With the estimates of PIA, its reliability, ζ, and the reliability of ε given in SRT and DSD modules, the most possible combination of PIA and ε satisfying Eq. (202) is selected as final estimates.

$$\mathrm{PIA} = -\frac{10}{\beta}\log_{10}(1-\varepsilon\zeta) \tag{202}$$

With the modified k-Z_e relationship ($k=\varepsilon\alpha Z_e^{\beta}$), attenuation correction is done again by Eq. (40) and the final estimates of Z_e is obtained.

(3) Processes at dual-beam pixels

(3-1) Target pixels and range bins

Pixels with precipitation and without any errors are processed. Echo region and noise region are

defined for each frequency as in (2-1). Storm top range bins may be different between the two frequencies. And do land surface range bins. The retrieval should be done between higher storm top range bins and lower surface range bins. Section I is from higher storm top range bin to lower storm top range bin, which is echo region for one frequency. Below section I, there may be echo region common to both frequencies. It is called section II. Below section II, echo region for only one frequency (section III) and common noise region (section IV) may exist. In case that lower echo bottom range bin is higher than higher storm top range bin, though it seems rarely occur, an exceptional procedure is required, and should be considered in near future.

(3-2) Retrieval

(3-2-1) Section I

For the frequency which has echo in section I, the single-beam retrieval process as shown in (2-2) is applied, and the results are adopted only for section I. For another frequency, attenuation in section I is calculated.

(3-2-2) Section II

In section II, dual-frequency retrieval can be applied. As the bottom of section II is generally not the land surface, backward retrieval method with SRT cannot be applied without extrapolation in section III and section IV. Then, forward retrieval method is applied. Actually, the iterative backward retrieval method, which is essentially equivalent to forward retrieval method, is used. The forward retrieval method and the iterative backward retrieval method generally have multiple solutions. For each solution, the next process (3-2-3) is executed.

(3-2-3) Sections III and IV

For the frequency which has echo in section III, the single-beam retrieval process as shown in (2-2) is applied in section III and section IV, by considering the attenuation caused in section I and section II.

(3-2-4) Selection of optimal solution

Among multiple solutions in (3-2-2), the solution of which ε estimated in (3-2-3) is closest to 1 is selected to be the final solution.

(4) Primary output physical variables

Primary physical variables output by Solver module is (N*, D*), Z_e, PIA, attenuation-corrected backscattering cross section σ^0_e, precipitation rate, and precipitation water equivalent.

In dual-frequency retrieval, (N*, D*) are estimated in prior to Z_e. On the other hand, in

single-frequency retrieval, Z_e is estimated in prior to (N^*, D^*). But, (N^*, D^*) and Z_e are easily converted to each other in Eq. (21) and (22). Please remember that PIA includes attenuation only by precipitation particles. σ^0_e is calculated as the sum of σ^0_m and PIA final estimates. By integrating drop size distribution and falling velocity, precipitation water equivalent and precipitation rate are calculated. ε is range independent at SB pixel and in Sections I, III, and IV at DB pixel. But, in section II at DB pixel, ε can be calculated by k and Z_e and is range dependent.

(5) RTM look up table

For the retrieval, $I_e(D^*)$ and $I_b(D^*)$ in Eqs. (31), (32), and (45) need to be quantified. They are the function of D^*, and also of $n(D; D^*)$, ε, and λ.

$I_e(D^*)$ and $I_b(D^*)$ can be calculated by Mie theory, but the time of computation is not negligible. To save the time, $I_e(D^*)$ and $I_b(D^*)$ are calculated with various conditions and the results are summarized in RTM look up table.

Below is an estimation of the size of RTM look up table. As long as Gamma distribution function is applied as drop size distribution function, only μ is variable for liquid precipitation, but μ and ρ_b are variables for melting and solid precipitation in the case of Eq. (114). If Eq. (115) is used, falling velocity affects the look up table. The number of steps for D^* is determined by considering the trade-off between the error caused by interpolation and the size of look up table. As ε is an complex number, the number of steps becomes large as (the number of steps for real part) times (the number of steps for imaginary part). Instead of ε itself, for possible combination of phase, density, and physical temperature, RTM look up table can be produced. For wavelength, only two steps are necessary.

In near future, the effect of non-spherical particles should be involved. The ellipsoid liquid particle can be relatively easily introduced. These effects are considered in the look up table without changing the source code as much as possible.

RTM look up table may be prepared not for $I_e(D^*)$ and $I_b(D^*)$ but for $\sigma_b(D)$ and $\sigma_e(D)$ so that the table can be applied for any type of drop size distribution function. The latter requires the integration in terms of D in Solver module and may take some more computation time.

(6) Update of SRT database (weak rainfall reference method)

Weak rainfall reference method is a kind of surface reference method and may be introduced in the L2 algorithm. Generally, SRT assumes that the land surface conditions are the same between no-precipitation condition and precipitation condition, but this assumption is not valid in many cases. Over land, the increase in surface soil moisture caused by precipitation can increase the surface backscattering cross section. Over ocean, as stronger wind is accompanied by precipitation, the incident angle dependence tends to be weaker under precipitation. Therefore, weak rainfall reference method summarized not σ^0_m under no-precipitation but σ^0_e under precipitation to be compared with σ^0_m under

precipitation.

Under precipitation, σ^0_e estimated in Solver module is categorized for different calendar month, lat./lon. grid, and incident angle as in the temporal reference method. The 0^{th}, 1^{st}, and 2^{nd} moment of σ^0_e are summarized into the database. As the number of precipitation pixels is much smaller than that of no-precipitation pixels, the grid size of weak rainfall reference method should be as large as 1.0 degree by 1.0 degree, for example. With this resolution, a few grids contains land and ocean (and coast) pixels, the database should be prepared separately for land, ocean, and coast.

When the precipitation rate is heavy, the error of PIA may be larger, so does the error of σ^0_e. Therefore, it may be better that σ^0_e only under weak rainfall is sampled and the name of the method is "weak" rainfall reference method. We need to examine the difference of land surface types between weak rainfall and heavy rainfall.

(7) Transfer of k-Z_e relation

In section II at DB pixel, ε can be calculated for each range. We would like to transfer ε to single-beam pixels to improve their k-Z_e relation. There may be largely two strategies. One is to find the dependence of ε on region, season, and height. This will enable us to improve DSD look up table. With early observations of DPR, DSD look up table is improved and used for later observations. Another is to transfer ε to neighboring single-beam pixels within the same orbit. Pixels in the same precipitation system may assume the same ε, but this assumption needs to be validated and actual procedure of transfer of ε should be developed.

3.2.7 Texture module

This module estimates the beamfilling inhomogeneity and reflectivity gradient within the field of view. It possibly uses interleaved Ka-band data in the central swath that provide denser sampling points in a horizontal surface. The inhomogeneity of rain distribution provided by this module is planned to be used to help correcting the effects of non-uniform beamfilling (NUBF) and classifying storm types. However, no concrete method has been developed yet. This module is likely to be added to the system in the later stage of the whole algorithm development.

4. VALIDATION (TEST AND VERIFICATION)

4.1 Pre-launch of the GPM core satellite

Before the launch of the GPM core satellite, we will test the algorithm test and physically validate it as much as possible with collaboration of the GPM GV team. In the algorithm test, algorithm mechanics and robustness will be checked. More than one type of test data will be needed. We will generate synthetic Ka-band data in the central swath from actual TRMM PR data (Ku-band) by assuming a relationship among the DSD parameters and the attenuation by clouds and water vapor. Airborne data (PR-2, APR-2) will provide realistic dual-frequency radar data although with many unknown parameters (e.g., clouds). Ground-based dual-frequency radars including NASA's dual-frequency and dual-polarized Doppler radar (D3R) and JAXA's dual Ka-band radar system will also provide realistic dual-frequency radar data. Synthetic data created by using a numerical model have an advantage that all parameters are known so that we can test the performance of the algorithm by checking whether the algorithm can retrieve the parameters correctly. Note that many parameters needed to reproduce radar echoes accurately are not handled well in most of the current numerical models. They include melting or partially frozen particles. Nevertheless, synthetic data created with simple assumptions are very helpful for sanity check of the algorithm.

In the physical validation, various parameters of the DPR algorithm will be tested with collaboration of the GPM GV team. The physical validation will validate the parameters in the physical model of the precipitation system assumed in the algorithm. They include the DSD parameters, density and shape of snow and melting particles, width and structure of the melting layer, supercooled droplets, attenuation by the water vapor and cloud, inhomogeneity of rain distribution and so on.

4.2 Post-launch of the GPM core satellite

After the launch of the GPM core satellite, product validation will be performed, in addition to the physical validation. Data taken nearly simultaneously by the GPM/DPR and the TRMM/PR enable us to make a direct comparison. Statistics such as averages and histograms of radar echoes taken by the DPR can be compared with the corresponding statistics of the TRMM/PR data. Ground instruments such as a dense rain gauge network and ground-radar including NASA's D3R and JAXA's dual Ka-band radar system can be used to validate the DPR products. Validations by using airborne data are desirable.

5. INTERFACE TO OTHER ALGORITHMS

The combined DPR-GMI algorithm requires outputs from the preparation module (PRE), the vertical profile module (VER), the surface reference technique module (SRT), and the classification module (CSF), in addition to the DPR radar reflectivity profiles. Precipitation detection from the PRE, pressure, temperature and humidity profiles from the VER, the PIA from the SRT, and bright band detection, altitude of the bright band (if it exists), and classification as convective or stratiform precipitation from the CSF will be used in the DPR-GMI combined algorithm.

The DPR products will be utilized also in the GPM Passive Microwave-Radar Enhanced Algorithm of an Optimal Estimation approach that uses the DPR/GMI data as the a-priori constraint.

6. ALGORITHM DELIVERY SCHEDULE

By the end of November 2011, the initial (version 2) algorithm should be prepared. The purpose of this algorithm is to check the overall flow of data. The initial algorithm needs to include the six modules with inputs and outputs as determined by the ATBD. The main (controller) module has only the basic procedure. Sub modules should include basic functions mentioned in ATBD excluding NUBF correction and other advanced functions. The scientific validity and the quality of the output are not questioned. Development (coding) of sub modules should start soon (from November 2010) and the first codes are submitted to DPR-L2 algorithm team by March 2011. Synthetic test data with simple assumptions are expected to be available by March 2011. Integration of sub modules (or developing the main module) and testing with the simple synthetic data will start in March 2011 and an early result of verification will be given in May 2011. From May to October 2011, improvement of algorithms and testing will be repeated in several times.

By the end of November 2012, the at-launch (version 3) algorithm should be prepared. In the at-launch algorithm, the main module may include advanced procedures such as the iteration of sub modules and processing with multiple conditions. NUBF and other advanced functions should be realized. Synthetic test data with realistic assumptions are expected to be available by March 2012. After the improvement of the main module, testing and improvement will be repeated by September 2012 and the final check will be done until November 2012.

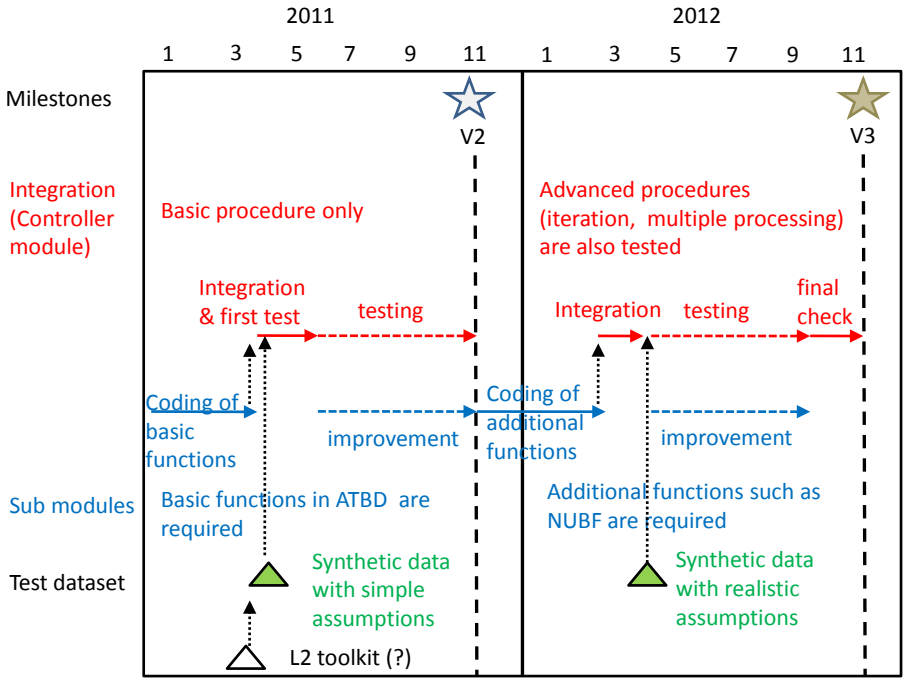

7. REFERENCES

Awaka, J., T. Iguchi, and K. Okamoto, "Early results on rain type classification by the Tropical Rainfall Measuring Mission (TRMM) precipitation radar," Proc. 8th URSI
Commission F Open Symp., Aveiro, Portugal, pp.143-146, 1998.

Awaka, J., T. Iguchi, and K. Okamoto, “TRMM PR standard algorithm 2A23 and its performance on bright band detection,” J. Meteor. Soc. Japan, 87A, pp.31-52, 2009.

Caylor I.J., G.M. Heymsfield, R. Meneghini, and L.S. Miller, 1997: Correction of sampling errors in ocean surface cross-sectional estimates from nadir-looking weather radar. *J. Atmos. Oceanic Technol*., **14**, 203-210.

Iguchi, T. and R. Meneghini, 1994: Intercomparisons of single-frequency methods for retrieving a vertical rain profile from airborne or spaceborne radar data. *J. Atmos. Oceanic Technol*., **11**, 1507-1516.

Iguchi, T., T. Kozu, J. Kwiatkowski, R. Meneghini, J. Awaka, and K. Okamoto, 2009: Uncertainties in the Rain Profiling Algorithm for the TRMM Precipitation Radar. *J. Meteor. Soc. Japan*, Vol. 87A, 1-30.

Kozu, T., 1995: A generalized surface echo radar equation for down-looking pencil beam radar. *IEICE Trans. Commun*., **E78-B**, 1245-1248.

Marzoug, M. and P. Amayenc, 1994: A class of single- and dual-frequency algorithms for rain rate profiling from a spaceborne radar. Part I: Principle and tests from numerical simulations. *J. Atmos. Oceanic Technol*., **11**, 1480-1506.

Meneghini, R., and T. Kozu, 1990: Spaceborne weather radar. Artech House (Boston/London), Norwood, MA, 197pp.

Meneghini, R. and K. Nakamura, 1990: Range profiling of the rain rate by an airborne weather radar. *Remote Sens. Environ*., **31**, 193-209.

Meneghini, R., T. Iguchi, T. Kozu, L. Liao, K. Okamoto, J.A. Jones, and J. Kwiatkowski, 2000: Use of the surface reference technique for path attenuation estimates from the TRMM Radar. *J. Appl. Meteor*., **39**, 2053-2070.

Meneghini, R., J.A. Jones, T. Iguchi, K. Okamoto, and J. Kwiatkowski, 2004: A hybrid surface reference technique and its application to the TRMM Precipitation Radar, *J. Atmos. Oceanic Technol.*, **21**, 1645-1658.

Onogi, K., J. Tsutsui, H. Koide, M. Sakamoto, S. Kobayashi, H. Hatsushika, T. Matsumoto, N. Yamazaki, H. Kamahori, K. Takahashi, S. Kadokura, K. Wada, K. Kato, R. Oyama, T. Ose, N. Mannoji and R. Taira , 2007 : The JRA-25 Reanalysis. *J. Meteor. Soc. Japan*, **85**, 369-432.

Press W.H. et al., 1992: *Numerical Recipes in FORTRAN, 2nd Edition.* Cambridge University Press. ISBN 0 521 43064 X.

Rosenkranz, P. W., 1975: Shape of the 5mm oxygen band in the atmosphere. *IEEE Trans. Ant. and Propag.*, AP-23, 498-506.

Seto, S. and T. Iguchi, 2007: Rainfall-induced changes in actual surface backscattering cross sections and effects on rain-rate estimates by spaceborne precipitation radar. *J. Atmos. Oceanic Technol.*, **24**, 1693-1709.

Steiner, M., R.A. Houze, Jr., and S.E. Yuter, "Climatological characterization of three-dimensional storm structure from operational radar and rain gauge data," J. Appl. Meteor., 34, pp.1978-2007, 1995.

Ulaby, F. T., R. K. Moore, and A. K. Fung, 1981: *Microwave Remote Sensing: Active and Passive.* Vol. I. Artech House, Norwood, MA, 456pp.

Waters, J.W., 1976: Absorption and emission of microwave radiation by atmospheric gases, in Methods of Experimental Physics, M. L. Meeks, ed. 12, Part B, *Radio Astronomy*, Academic Press, Section 2.3.

8. ACRONYMS

BB:	Bright band
CSF module:	Classification module
NP-attenuation:	Attenuation due to non-precipitation particles
PRE module:	Preparation module
SLV module:	Solver module
VER module:	Vertical module